National Research FLAGSHIPS
Wealth from Oceans

CSIRO

Remote sensing of previously unmapped marine habitats on the south coast of Western Australia

E.J. Botha, A.G. Dekker, YJ Park.
26th May 2009

Prepared for:
WA Department of Environment and Conservation (DEC), South Coast Natural Resource Management Inc. (South Coast NRM), South West Catchments Council (SWCC)
Contact: Ewan Buckley (WA DEC)

Enquiries should be addressed to:
Hannelie Botha
Environmental Earth Observation
CSIRO Land and Water
GPO Box 1666, Canberra ACT 2601
Tel. 02 6246 5744
e-mail: elizabeth.botha@csiro.au

Distribution list

WA Department of Environment and Conservation (DEC)	[Insert copies received]
South Coast Natural Resource Management Inc. (South Coast NRM)	[Insert copies received]
South West Catchments Council (SWCC)	[Insert copies received]

Copyright and Disclaimer

Important Disclaimer

Contents

List of Figures

List of Tables

1. BACKGROUND

In September 2006 the Western Australia (WA) State Government instigated the South Coast Regional Marine Planning (SCRMP), a multi-agency project led by the WA Department of Environment and Conservation (WA DEC) to produce a strategy to guide marine planning along WA's south coast, from the WA/SA border to Cape Leeuwin. One of the SCRMP aims is to characterise environmental, social, economic and cultural values and inter-sectoral issues and impacts for the region, through advice from community members and government agency representatives. The SCRMP is also operating in cooperation with the Commonwealth Marine Bioregional Planning process currently underway in the South West Bioregion.

A sound spatial (GIS-based) information base was required to support the SCRMP process, and with funding from South Coast Natural Resource Management (NRM), the WA DEC initiated a project to collate or produce this information using satellite imagery, required for regional marine planning, with later funding contributions from South West Catchments Council (SWCC). This project established that a significant gap existed in available data of marine habitat mapping along the south coast, with approximately half of the planning region having no broad scale habitat mapping information available.

In order to address this information gap, it was decided to demonstrate the feasibility of using best-practice remote sensing methods developed by CSIRO Environmental Earth Observation Group to derive the best possible community-level habitat mapping for two high spatial resolution images and one moderate spatial resolution image on the south coast. This best-practice remote sensing method can provide broad-scale image thematic maps without necessitating highly detailed *in situ* measurements. These mapped areas will provide information to a broader assessment of the distribution of various marine habitats across the south coast of WA.

2. PROJECT OBJECTIVES

This project aimed to map coastal marine benthic habitats of selected areas along WA's south coast, using the expertise of the CSIRO Environmental Earth Observation Group's aquatic research team. Satellite imagery was pre-processed to correct for sunglint and atmospheric effects to produce subsurface remote sensing reflectance images. The sun glint and atmospheric correction is an essential pre-processing step for a physics-based image processing approach. Subsurface remote sensing reflectance images were subsequently processed using the Semi-Analytical Model for Bathymetry, Un-mixing and Concentration Assessment (SAMBUCA). SAMBUCA estimates water column constituent concentrations, water column depth and benthic substrate composition from remote sensing data, and is thus able to deliver a bathymetric model and benthic substrate map from suitable satellite images.

Specific objectives included:

- Reviewing the suitability of existing high resolution satellite imagery to implement the SAMBUCA semi-analytical habitat mapping technique.

- Collect a limited amount of *in situ* measurements of substratum or substratum cover reflectance using non-submersible field spectrometers. A thematic gap in spectral data availability for the WA south coast was identified by the National Land and Water Resources Audit (NLWRA). The collection of spectral reflectance data of subtidal substratum, sea grass and macro-algae cover, harvested from the beach and intertidal rocks, will thus not only enhance the results possible for this project but will also contribute to the coastal spectral library being developed nationally.

For each image/area the intention was to deliver:

- Processed imagery with modeled atmospheric, sea surface and water column constituents removed (as possible) – i.e. images enhanced for identifying marine substrata

- Image classification – to maximum thematic resolution (e.g. to functional or community level habitats - sand/seagrass/macroalgae/reef/other; or more detailed as possible – genera, species, etc).

- Modelled bathymetry for the areas mapped

- Maximum optical depths over the image areas (an assessment of water column depth beyond which no measureable signal from the substratum reaches the water surface).

3. METHODS

3.1 Study sites

Two study sites were selected to address the lack of habitat mapping in their respective areas. Each site is relatively remote and/or difficult to survey using boat-based methods due to their distance from safe anchorages, and the often-inclement weather experienced in the south coast region of WA. These study areas were:

1. An area west of Red Rocks Point, along Middini Beach in the remote Roe Plains coast (Figure 1). This site falls within a broader coastal compartment stretching from Eucla to Scorpion Bight for which there is no habitat maps available. It was expected that information from remote sensing substrate mapping will add significantly to the understanding of the coastal marine environment in this region.

2. An area west of Broke Inlet on the coast between Walpole and Windy Harbour (Figure 1). This site abuts the Broke Inlet study site of the Securing WA's Marine Futures project (http://marinefutures.com.au/index) thus providing a potential comparison between boat-based and remote sensing methodologies. Boat-based methods in this region are limited to a minimum safe working depth of 10-15m, depending on proximity to the coast and weather conditions. Remote sensing imagery can provide complementary information to such habitat mapping projects, as it is most effective in shallow waters to where the reflectance of the substratum is no longer visible at the water surface. This depth of substratum information fluctuates with water column turbidity but often varies between six and twelve meters in clear coastal water.

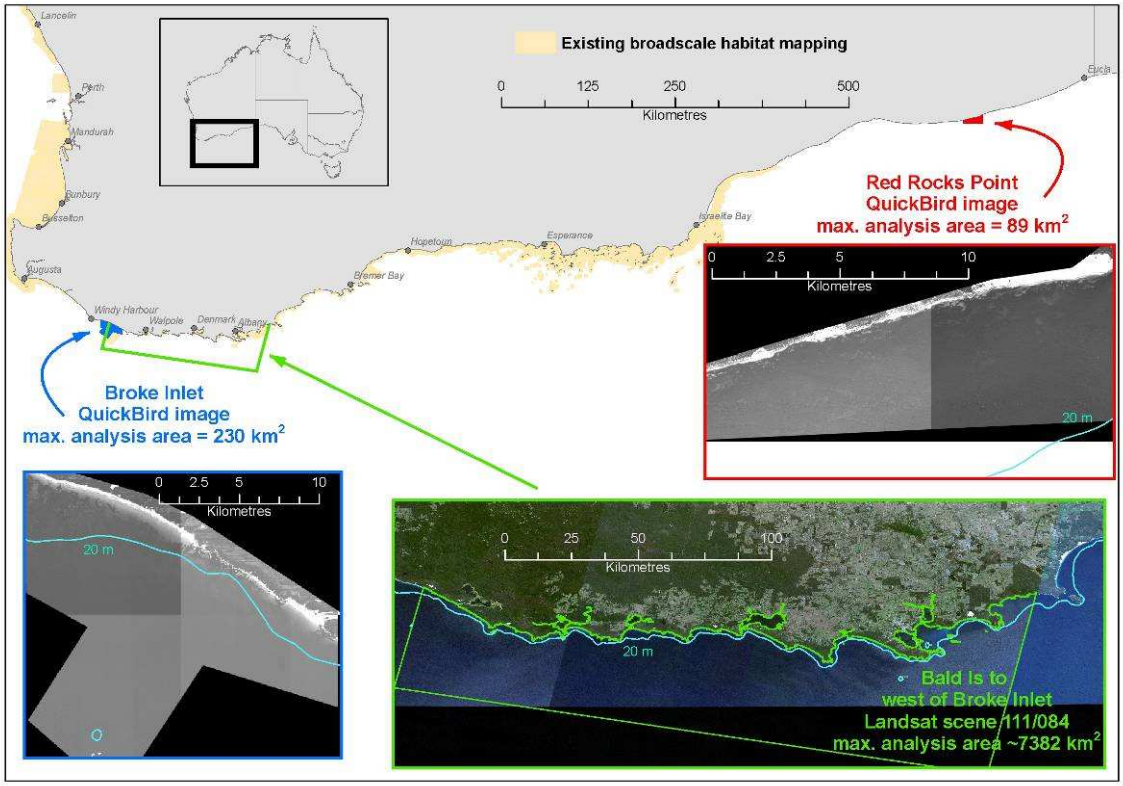

Figure 1 Study areas indicating the extent of the satellite image coverage (image source: WA DEC)

3.2 Field data collection

To properly parameterize the physics-based model implemented in this project, the optical properties of the substratum and the water column are required. Ideally, a comprehensive field data collection campaign should include optical measurements to describe downwelling irradiance, upwelling radiance, absorption, attenuation and backscattering of light in the water column and the spectral properties of the underlying benthos. However, this project was intended to explore the possibility of implementing a physics-based classification approach using a parameterization based on the best-fit optical properties available for the study site. Therefore the optical properties of the water column were parameterized using data collected at Cockburn sound during a field data collection campaign in 2003.

Whilst it was not possible to conduct field data collection in the Red Rocks Point area, due to the limited scope in budget and time of this project, a two-day site visit was conducted in November 2008 at sites that were within the area covered by the Landsat scenes acquired for this study. Two coastal sites were visited (Figure 2), one in the D'Entrecasteaux National Park (Fish Creek/West Cliff points) close to Broke Inlet and one in the Two Peoples Bay Nature Reserve near Albany. Substratum samples were collected on the beach and by snorkel-based harvesting in Two Peoples Bay. Reflectance spectra were measured with an ASD FieldSpec Pro HandHeld spectrometer, on loan from Geoscience Australia through the NLWRA. Spectral data that was collected were essential for the results and were also added to the coastal spectral library being developed nationally. Figures 3 and 4 shows examples of selected substratum spectra collected at the field sites. Where the spectra are clearly separable there is a better

likelihood of being able to map the associated species; whereas where the spectra are similar, discrimination will become less certain.

Adverse conditions at the Fish Creek site prevented safe swimming. It was thus not possible to collect *in situ* substratum samples at the Fish Creek site. Instead spectra were collected from benthic vegetation types that were washed-up on the shore. In addition to aquatic vegetation spectra, sand, rock and terrestrial vegetation spectra were collected at two sites east and west of West Cliff Point. Pseudo invariant feature (PIF) measurements were collected (as a radiometric and spectral calibration feature) of a nearby sand dune which is visible on the Landsat images. The Two Peoples Bay site was more sheltered and conditions were calm enough to allow snorkelers into the water to collect substrate samples for spectral measurements. This two day fieldwork (without needing boats and/or scuba gear and associated efforts) was considered to be an effective initial way to initiate the gathering of relevant spectral data.

The snorkeling fieldwork in Two Peoples Bay actually led to the possible discovery of a new *Riphillia* species which was harvested for spectral measurements as its color differed from the surrounding macro-algae and sea grasses. A sample has been sent to Belgium for DNA sequencing and a formal description.

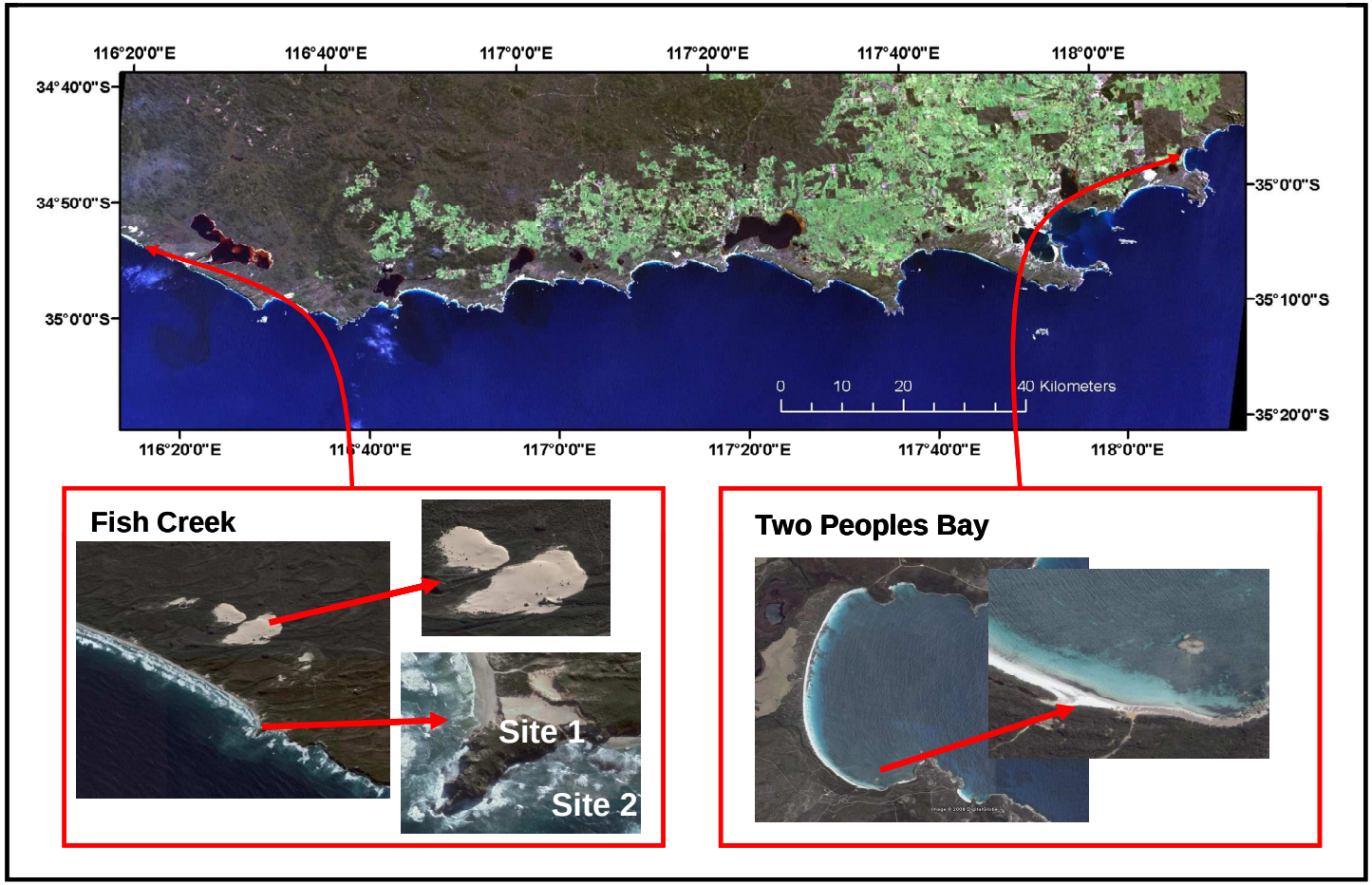

Figure 2 Landsat 7 ETM+ image of a portion of the Western Australian south coast (refer Figure 1) showing the locations of the field sites (Fish Creek and Two People's Bay) visited for data collection in November 2008.

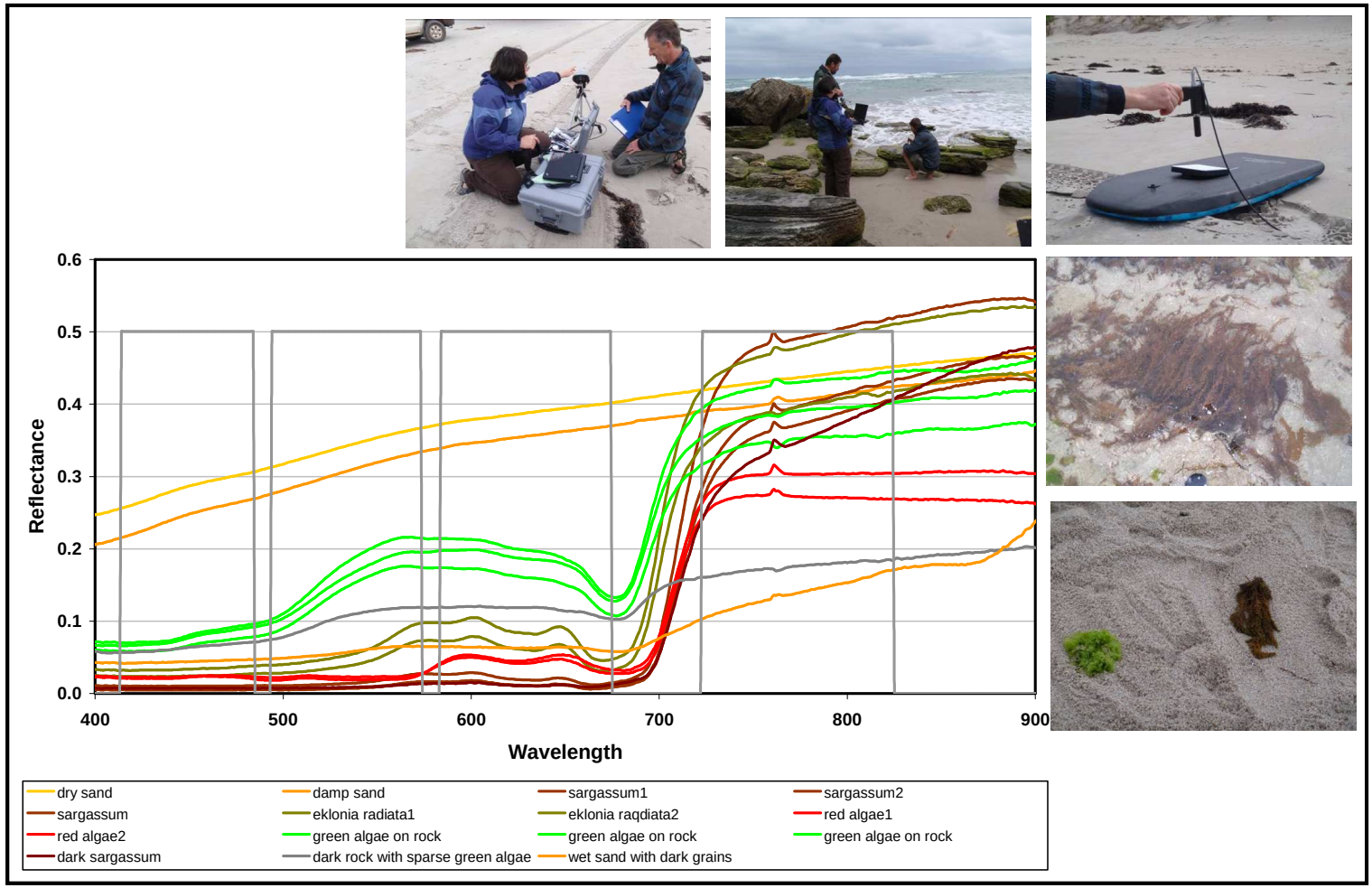

Figure 3 Substratum spectra collected with an ASD FieldSpec Pro HandHeld spectrometer (350-1100nm) in the D'Entrecasteaux National Park (Fish Creek/West Cliff points) close to Broke Inlet. Gray lines indicate the approximate extent of the satellite spectral bands. Within each spectral band the spectrum is averaged to one value only for that band. The ASD spectra have hyperspectral resolution whereas the QuickBird spectra have low spectral resolution.

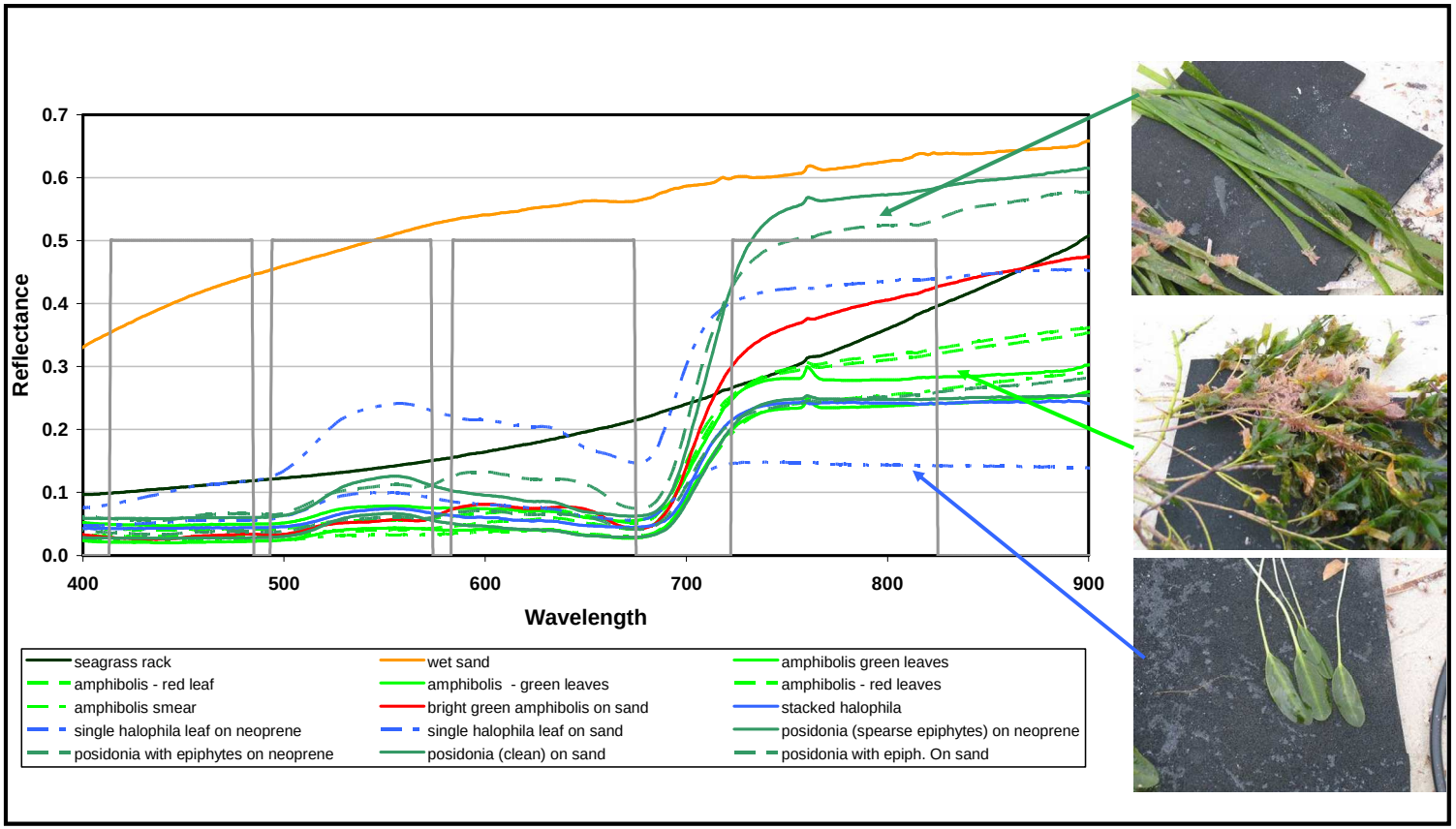

Figure 4 Selected seagrass spectra collected with an ASD FieldSpec Pro HandHeld spectrometer (350-1100nm) in the Two Peoples Bay National Park. Gray lines indicate the approximate extent of the satellite spectral bands

3.3 Image acquisition

The first objective of this study was to evaluate the suitability of archival satellite data of the study sites for habitat mapping purposes. Two QuickBird and two Landsat images were either available or purchased by WA DEC for use in this project (Table 1).

There were only a few QuickBird images of the proposed study sites available in the DigitalGlobe image archive due to their remote location. Digital Globe only rarely collects data over remote areas unless they are tasked and funded to do so. Cloud-cover, high amounts of sun glint and the need of some optically deep water in the scene to calibrate atmospheric correction, further limited the number of images that could reasonably be used for habitat mapping using the physics-based inverse semi-analytical modeling. Two QuickBird images, one of Broke Inlet and one of Red Rocks Point (see Table 1), were purchased for processing. Two additional Landsat images, both covering the same scene (Path/Row ID: 111/084), were also sourced by WA DEC for use in this project (Table 1). Due to the high amount of sun glint and sensor striping affecting the Landsat scenes, one additional, less glinted, Landsat scene of the same area was sourced by CSIRO from NASA (http://edcsns17.cr.usgs.gov/EarthExplorer/) for possible processing. However, this image acquisition on 14 August 1999 coincided with a period when large amounts of tannin-rich water were discharging from the estuaries and inlets into the coastal waters, causing significant variability in the water column (See Figure 7c and Figure 16). It was decided not to process the image for this project.

Table 1 Satellite images acquired for image analysis

Sensor	Coverage	Acq. date	Spatial res.	Comments	
QuickBird	Broke Inlet	03/03/2002	2.6m	Strong sensor banding and sun glint effects	Figure 6
QuickBird	Red Rocks Pt.	27/03/2005	2.9m	Sun glint affected	Figure 5
Landsat 5	Bald Isl. to Broke Inlet	11/02/1999	30m	Strong sensor striping and sun glint effects	Figure 7a
Landsat 7ETM+	Bald Isl. to Broke Inlet	06/02/2000	30m	Sun glint affected	Figure 7b
Landsat 7ETM+	Bald Isl. to Broke Inlet	14/08/1999 [1]	30m	High concentration of tannins discharging from estuaries causing variable water column properties	Figure 7c

[1]Additional image, sourced by CSIRO from NASA (http://edcsns17.cr.usgs.gov/EarthExplorer/) as a less glint affected alternative

3.3.1 Data quality

Prior to image-processing each image was assessed to determine the level to which it can be processed for creating thematic maps. Both image radiometric quality and environmental influences (atmosphere, sun and sky glint produced by swell and waves) were considered.

The two QuickBird images (Figure 5 and Figure 6) contained high amounts of sun-glint, affecting all the multispectral bands (but especially the Near Infrared band) due to strong wave-action and large swells. The Red Rocks Point image (Figure 5) also has large areas of very dark (probably vegetated) target, with only the Green and the Blue bands of the multispectral image effectively discriminating the target spectral characteristics. This resulted in only brighter sandy patches being reliably classified during the image analysis stage.

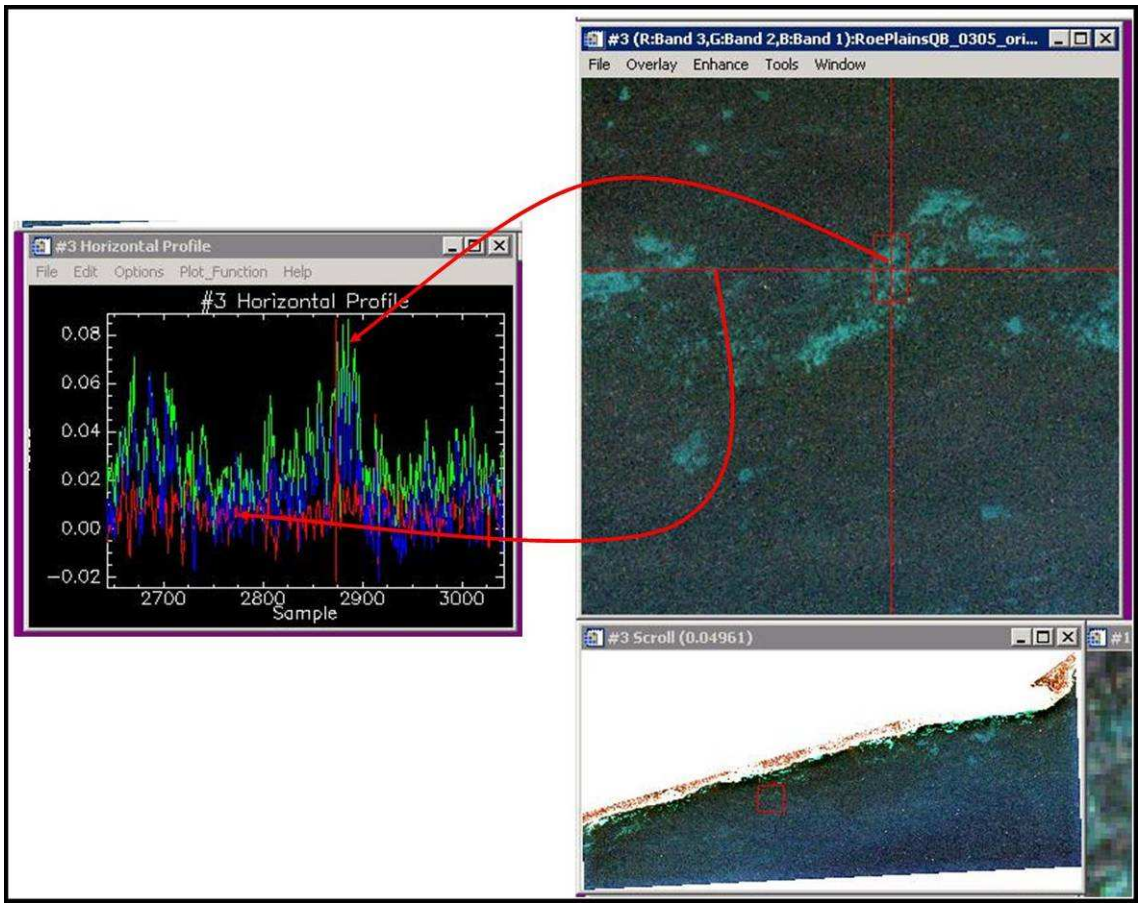

Figure 5 True colour QuickBird image of Red Rocks Point illustrating the spectral discrimination between the blue, green and red image bands. The top image is a zoom of the red square in the lower image. Brighter targets within the scene have a greater spectral separability than darker targets. The colours of the horizontal profiles reflect the actual colour of the spectral bands of the QuickBird satellite image (Blue, Green and Red). The spikiness in the horizontal profile of the image is the amount of noise due to sun glint (directly from the sun) and of waves reflecting skylight. Where the image crosses sand patches the reflectance clearly goes up (to 0.08 fraction reflectance or 8% reflectance)

In addition to environmental factors, such as sunglint, the Broke Inlet image (Image 6) also displayed vertical banding. This banding is an artefact of a post image collection uniformity correction applied by DiditalGlobe to improve the appearance of the image product. QuickBird image products are optimized for radiometric image quality over terrestrial targets (Krause 2004; Krause 2006) which compromises the radiometric integrity of aquatic targets in some cases. It should also be noted that the algorithm and radiometric calibration parameters applied to QuickBird images acquired prior to June 2003, such as the Broke Inlet image, are more

compromised than later acquisitions. As CSIRO applies a physics based atmospheric and air-water interface correction and processing method this radiometric uncertainty affects the results. CSIRO is currently communicating with Digital Globe engineers to clarify this issue and will spend some time in the near-future researching strategies to improve the processing pathway to deal with this source of error.

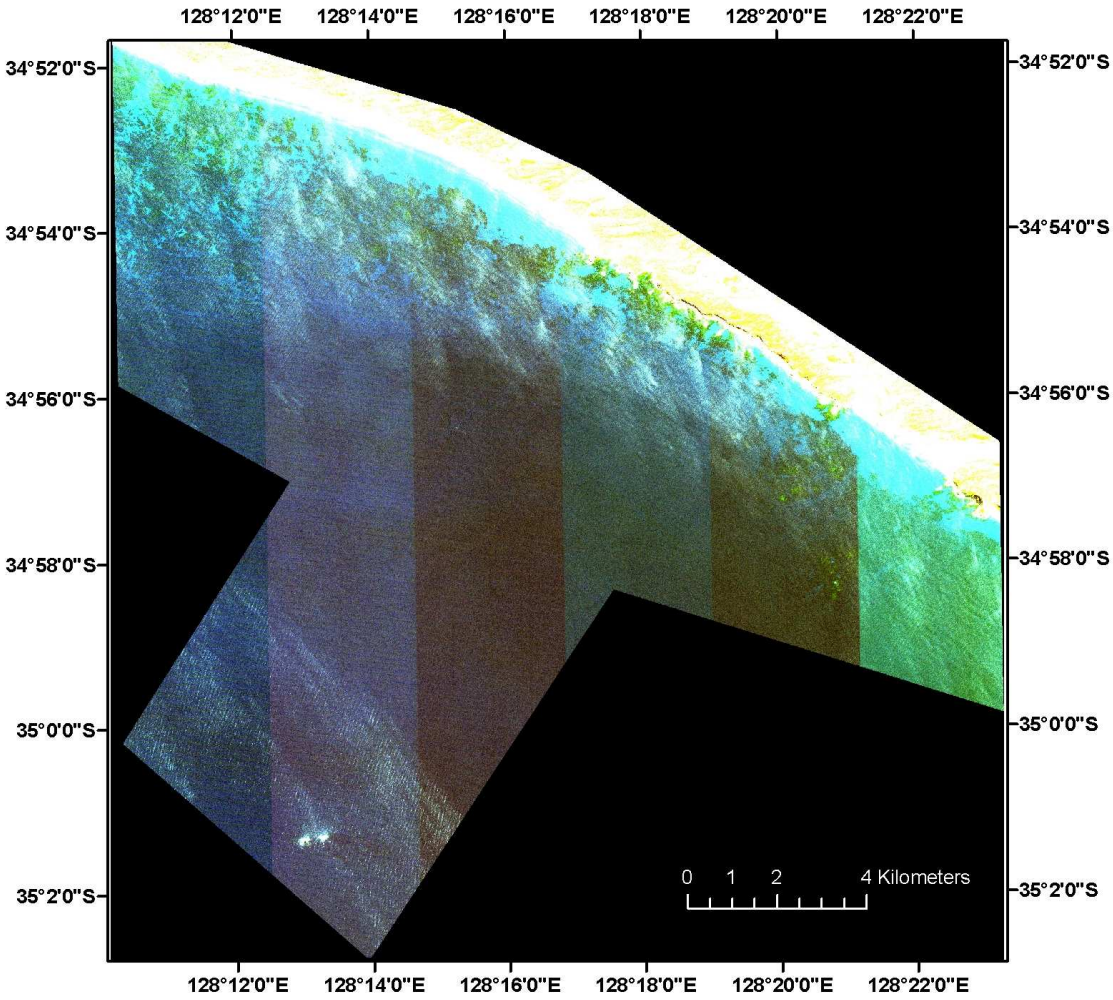

Figure 6 True colour QuickBird image of the coastline close to Broke Inlet illustrating the effects of sensor banding as well as areas in the scene that is optically shallow enough to allow substratum mapping. The two bands on the eastern-most side of the image differ by up to 1% in the green band which, considering that the information-content of the water-leaving radiance in the green band is below 5%, can contribute to significant analysis errors.

Both Landsat images acquired by DEC (Figure 7a and 7b) had large amounts of sunglint in the eastern portion of the image. The Landsat 5 image (Figure 7a) also had significant sensor-striping in the ocean part of the image, compromising the effectiveness of the physics-based image analysis approach. It was decided not to analyse the Landsat 5 image due to this issue. Additionally, the Landsat images that were sourced from Landgate appeared to have a radiometric correction applied to the green band that did not match the Landsat radiometric

calibration files used in the CSIRO physics-based atmospheric correction protocol. The selected Landsat image was thus atmospherically corrected using a standard empirical line correction technique instead.

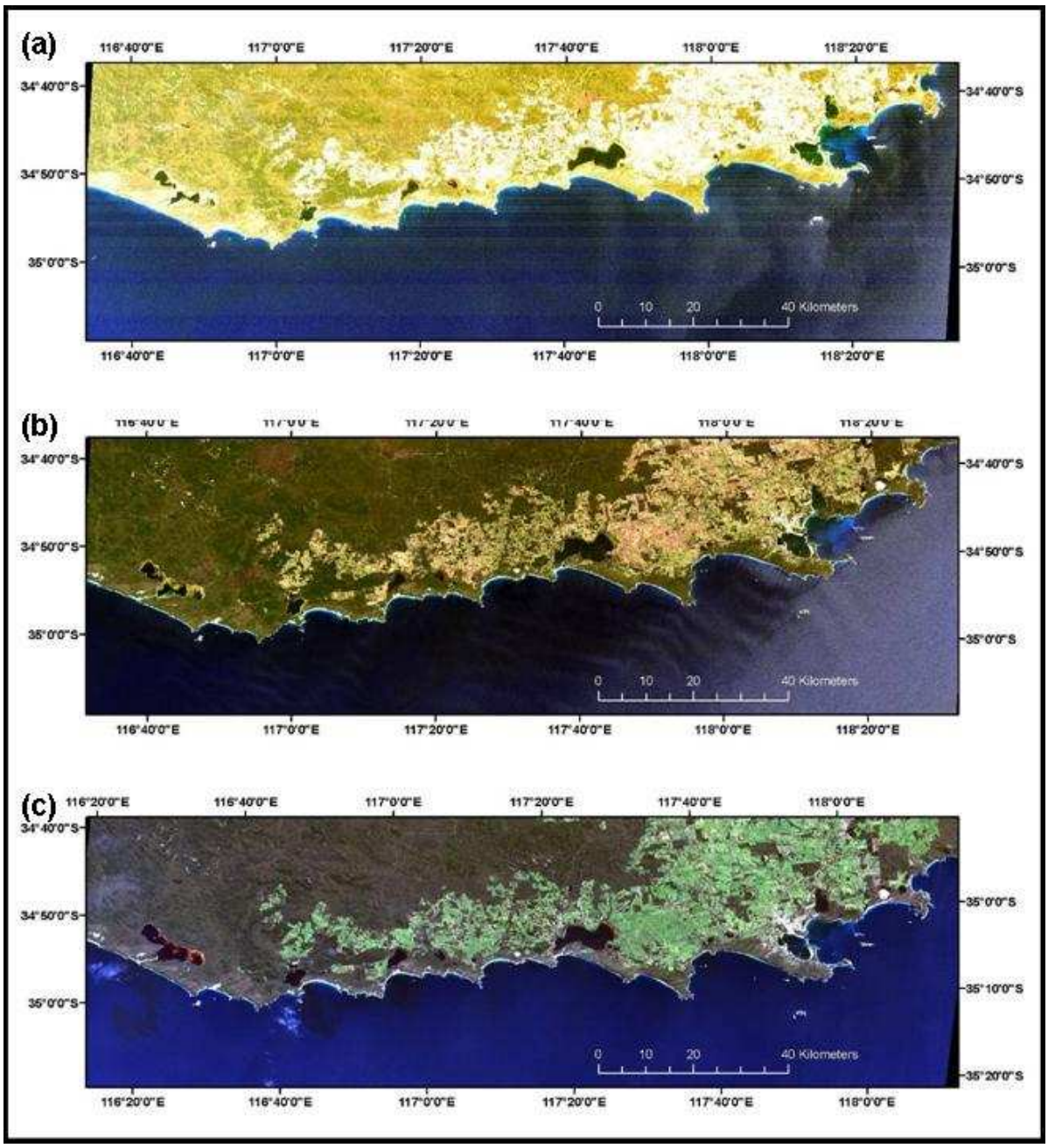

Figure 7 Landsat scenes (Path/Row ID: 111/084) available for the Broke Inlet to Bald Island section of the WA south coast. (a) Landsat 5TM scene acquired on 11/02/1999 that is affected by horizontal banding and some sun glint features in the Eastern side of the image, (b) Landsat 7ETM+ scene acquired on 06/02/2000, affected by sun glint in the eastern portion, and Landsat 7ETM+ scene acquired on 14/08/1999 that shows tannin rich plumes flowing into the coastal waters from the tannin rich lakes (ICOLLS).

3.4 Image Processing

Similar to the approach outlined by (Brando et al. 2009), an enhanced implementation of the inversion/optimization approach by (Lee et al. 1999; Lee et al. 2000) was applied to the multispectral satellite imagery. The approach was used to estimate bathymetry, substratum composition (i.e. fractional cover of e.g. sand, seagrass and macro-algae) and the concentrations of the optically active constituents of the water column, including chlorophyll, coloured dissolved organic matter (CDOM) and non algal particulate matter (NAP). Figure 8 presents the schematic flowchart of the integrated physics based mapping approach that includes atmospheric correction and an objective process of quality control.

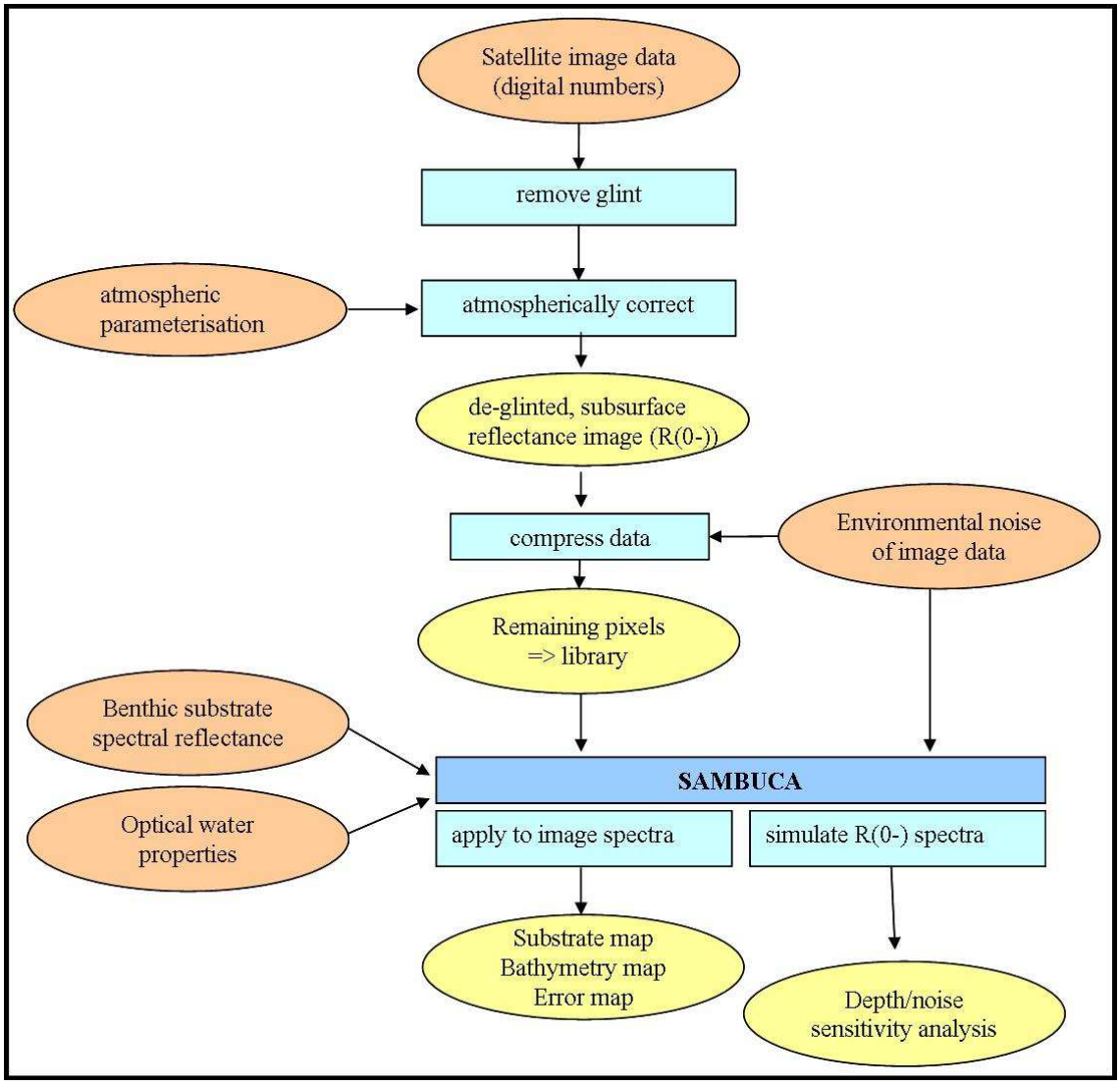

Figure 8 Workflow for investigating substratum type using a physics-based approach on Quickbird and Landsat image data. This approach allows multitemporal and multi sensor comparison for information derived from remote sensing data.

3.4.1 Glint removal

High spatial resolution satellite images over water bodies are often affected by specular (mirroring) surface reflection of incident sun light, called sun glint, as well as sky glint (the diffuse blue light) which impedes the accurate assessment of water leaving radiance thus affecting the accuracy and validity of the mapping of water depth, water column composition and benthic habitats. As a first step in the integrated physics-based mapping approach (Figure 8), glint is removed from the image as far as possible.

An approach to remove this sun glint has been developed by (Hochberg et al. 2003) and refined by (Hedley et al. 2005). This approach assumes negligible water reflectance at a near infrared (NIR) band. However, this assumption is not true if water column is shallow, where the water leaving reflectance is affected by the bottom reflectance. Consequently, this approach would overcorrect the glint for shallow water pixels. (Vahtmae and Kutser 2008) proposed another sun glint correction algorithm, which utilizes the absorption feature due to atmospheric oxygen at 760nm. Since this algorithm requires a fine spectral resolution around the oxygen absorption band, it can not be applied to satellite imagery from low spectral resolution satellites such as QuickBird and Landsat. Therefore, there is a need to develop a glint correction algorithm, which maintains non-negligible NIR reflectance in shallow water pixels and is applicable for spectrally low (but spatially high resolution) imagery. For this purpose, we utilize the nature of spatial inhomogeneity of the sun glint patterns. There are two steps – 1) estimation of the sun glint spectral shape function and 2) sun glint estimation and correction for each pixel.

Spectral shape function of the sun glint

The satellite measured reflectance, ρ_t, consists of the atmospheric column reflectance, ρ_{atm} and the glint reflectance, ρ_g, and the water leaving reflectance, ρ_w.

$$\rho_t = \rho_{atm} + \rho_g + \rho_w \quad (1)$$

The glint reflectance, ρ_g for pixel p_i can be expressed:

$$\rho_g(p_i) = r_F(p_i) \cdot T(\lambda), \quad (2)$$

where $r_F(p_i)$ is Fresnel reflectance for the pixel p_i and $T(\lambda)$ is two-way atmospheric transmittance. The Fresnel reflectance due to air-water interface is almost spectrally constant in the visible to near-infrared range.

In order to estimate the spectrum of sun glint, we select an area of the image where atmosphere and water optical properties are relatively homogenous. A good example of the homogenous area is a deep water part. Within the homogenous area, the reflectance difference between pixel p_i and pixel p_j is due to the difference of glint reflectance.

$$\Delta\rho_t = \rho_g(p_i) - \rho_g(p_j) \quad (3)$$

Since the atmospheric transmittance is constant over the homogenous area, this can be written as:

$$\Delta\rho_t = (r_F(p_i) - r_F(p_j)) \cdot T(\lambda) \quad (4)$$

From this equation, we get a spectrum that is proportional to the atmospheric transmittance, $T(\lambda)$. By taking an average of these spectra over pixels within the area and then normalizing at NIR band, we obtain the spectral shape function for the glint reflectance. This glint spectral shape function is applied for the entire image.

Sun glint magnitude estimation and correction for each pixel

Within a box (with appropriate size, 3 by 3 in this study), we assume that the pixel of minimum reflectance is free of the glint effects. We take a boxcar average for the minimum reflectance in 2-D space to get a smoothed glint-free reflectance. The spatial smoothing elevates the low values of the minimum reflectance which is often associated with wave shades. This computation is done for the NIR band reflectance. Following this, the glint reflectance at the NIR band for each pixel is estimated by subtracting the glint-free reflectance from the reflectance of the pixel. Finally, by multiplying the glint spectral shape function described above, the glint reflectance spectrum for each pixel is computed and is subtracted from the measured spectrum.

3.4.2 Atmospheric and air-water interface correction

Atmospheric correction of the satellite imagery using c-WOMBAT-c

As the second step of the integrated physics based mapping approach (Figure 8), the ‘coastal Waters and Ocean MODTRAN-4 Based ATmospheric correction’ (‘c-WOMBAT-c’) procedure (Brando and Dekker 2003; Phinn et al. 2005) was applied to achieve atmospheric correction of the satellite imagery. The procedure combines an atmospheric inversion from at-sensor-radiance to above water reflectance (Adler-Golden et al. 1998(Adler-Golden et al. 1998a; De Haan et al. 1997) with an inversion of the air-water interface from above water reflectance to subsurface reflectance (De Haan and Kokke 1996; De Haan et al. 1997).

c-WOMBAT-c applies a full MODTRAN-4 atmosphere parameterisation and characterisation to retrieve the subsurface remote-sensing reflectance *R0-*. The atmospheric parameterisation for each QuickBird image was based on radiosonde data from the Australian Bureau of Meteorology Station at Esperance (for the Red Rocks Point QuickBird image) and Albany (for the Broke Inlet QuickBird image) to estimate the atmospheric column water contents. The estimate of ozone content was downloaded for the dates of satellite overpasses from the Total Ozone Mapping Spectrometer – TOMS database (http://toms.gsfc.nasa.gov/ozone/ozone.html).

Table 2 Atmospheric parameterization used to convert the QuickBird data to remote sensing reflectance

Model parameter	Red Rocks Point	Broke Inlet
Model atmosphere	midlatitude summer	Midlatitude summer
Albedo	0.05	0.05
H_2O (cm)	3.02	1.82
O_3 (DU^{-10})	0.26	0.26
Aerosol model	Navy Maritime (near shore)	Navy Maritime (near shore)
Visibility: (km)	50	100
Sensor altitude(km)	450	450
Sensor zenith (degrees)	168	154
path azimuth (degrees)	257.4	61.10
Day number of year	86	62
Target Latitude (dec. deg)	-32.194	-34.85
Target Long. (360-W)	232.66	243.83
Dec. Greenwich Time	1.87	2.32
Spectral range(nm)	400-1000	400-1000

In c-WOMBAT-c, atmospheric adjacency effects from photons transferring from adjacent higher reflecting pixels to the one being sampled are corrected for by using an averaged surface radiance for the surrounding region. This spatially weighted image is generated by convolving the input radiance imagery with a one square kilometre spatial weighting function (Adler-Golden et al. 1998b).

Empirical Line Correction (ELC)

CSIRO received radiometrically corrected and geopositioned Landsat files which originated from LandGate in WA. Despite best efforts using C-WOMBAT-C, a radiometric calibration issue was found in the green band of the Landsat image preventing the use of CSIRO's standard methodology. For expediency's sake, a standard empirical line correction (ELC) technique was used to atmospherically correct the Landsat scene. The ELC implements a linear regression between spectral data in the scene to match selected field reflectance spectra for each band equating DN and reflectance (Moran et al. 2001). This is equivalent to removing the solar irradiance and the atmospheric path radiance, producing apparent surface reflectance (Rapp). The technique requires at least one field, laboratory, or other reference spectrum and could be implemented for the Landsat images because targets measured during the field campaign were visible in the Landsat scene (figure 9). The apparent atmospheric correction was validated using additional spectra measured from terrestrial targets on the coast (Figure 10) thus illustrating the value of collecting a representative spectral library.

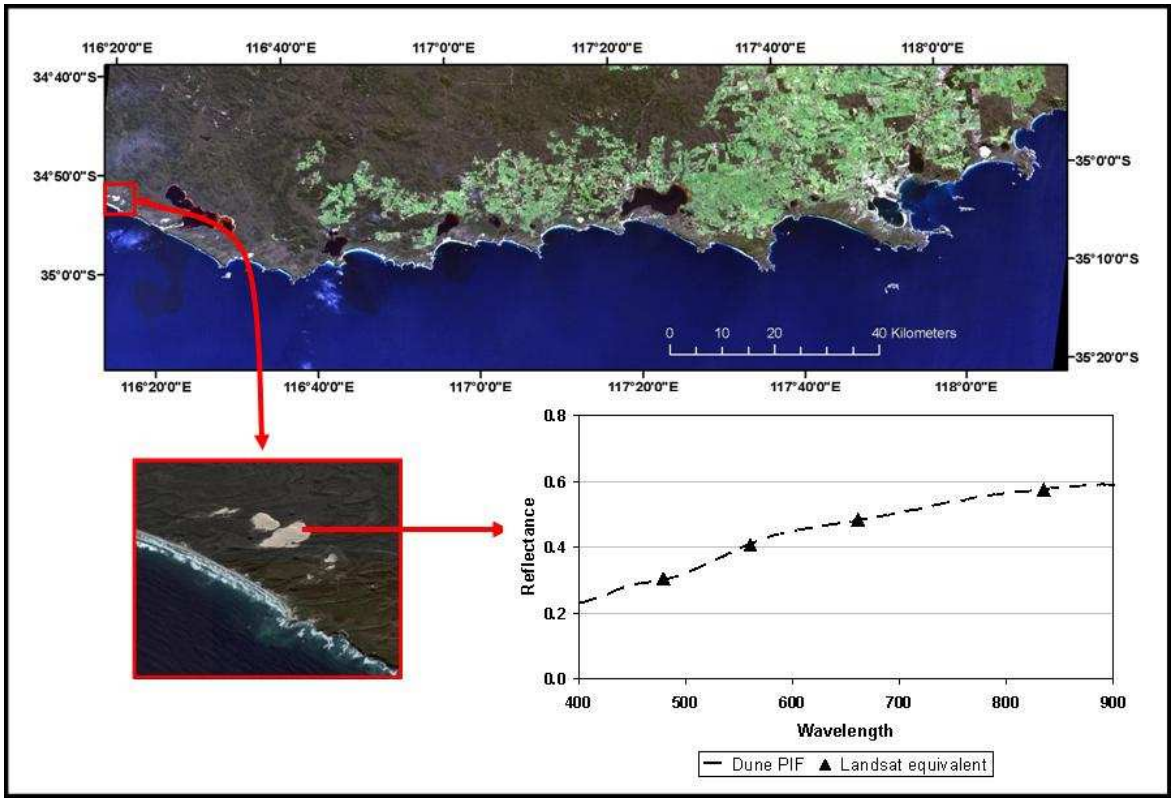

Figure 9 Location and field measured spectral signature of the large dune (Dune PIF) used as a pseudo-invariant target to atmospherically correct the Landsat scene. Triangular symbols on the graph indicate the Landsat-equivalent multi-spectral reflectance of the hyperspectral signal measured in the field.

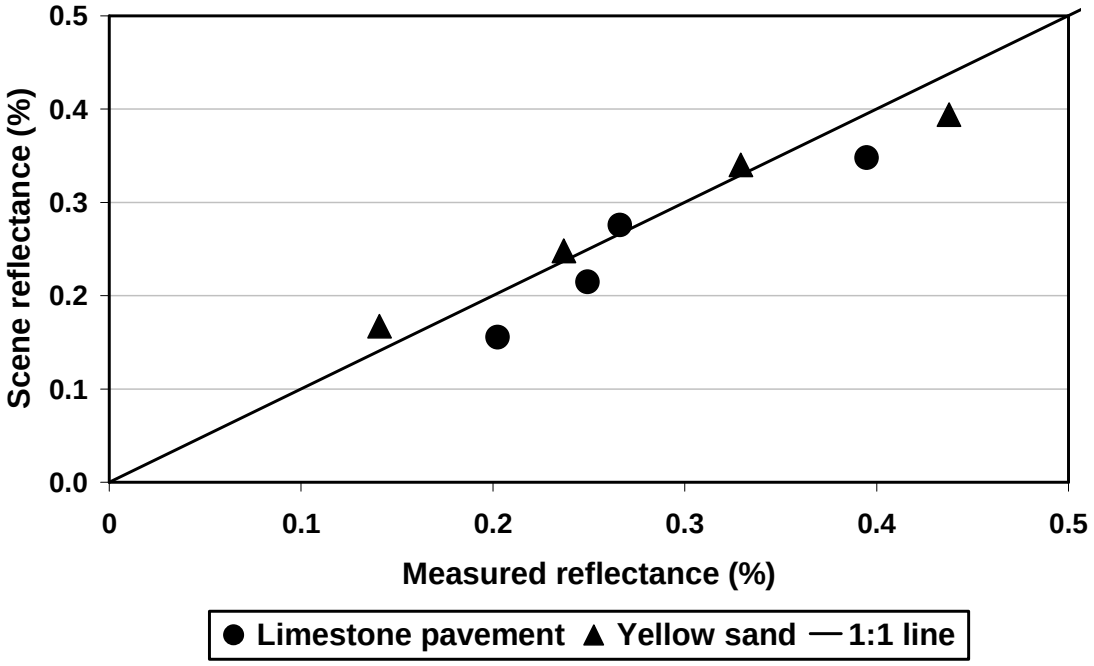

Figure 10 Scatter plot of *in situ* spectral reflectance (measured reflectance) and image-derived reflectance (scene reflectance) of two targets (yellow sand and limestone pavement) visible in the Landsat scene used to validate the empirical line atmospheric correction protocol.

An air/water interface correction, consistent with the c-WOMBAT-c model (Brando and Dekker 2003), was applied to the Rapp data to retrieve subsurface irradiance reflectance (R0-).

$$R(0-) = \frac{d_1 + d_2 R_{app}}{d_3 + d_4 R_{app}} \quad (5)$$

where d1, d2, d3 and d4 are the interface correction parameters which will differ for each spectral band. Specific correction values for the Landsat spectral bands used in this project are listed in Table 3.

Table 3 Air/water interface correction parameters applied through eq. 1 to the Landsat scene to retrieve subsurface irradiance reflectance from the atmospherically corrected apparent reflectance values

	d1	**d2**	**d3**	**d4**
Band 1	-0.0031	1	0.4176	0.48
Band 2	-0.0022	1	0.4191	0.48
Band 3	-0.0015	1	0.4201	0.48
Band 4	-0.0010	1	0.4210	0.48

3.4.3 Data volume reduction

Environmental dynamic range

In order to understand the precision and accuracy that can be achieved in the estimate of an environmental variable derived from reflectance with satellite imagery, it is necessary to estimate the overall sensitivity of the entire sensor-atmosphere-air-water interface system for detecting changes in reflectance. The environmental noise equivalent subsurface reflectance difference NE$\Delta R0$- provides an integrated measure of sensor signal–to-noise ratio and scene-specific characteristics such as the atmospheric variability and effects from the air-water interface (Brando and Dekker 2003). The NE$\Delta R0$- is estimated in the deepest waters in the imagery at the location identified as being the most homogenous using the methodology described by (Wettle et al. 2004). Figure 11 shows the NE$\Delta R0$- for each of the images involved in the analysis.

The values for NE$\Delta R0$- are quite large, indicating a poor signal to noise ratio. As remote sensing of submerged materials at the bottom of a water column requires separation of subtle spectral features the values of NE$\Delta R0$- ranging from 0.5% to 1% reflectance indicate that these images will not allow very accurate separation of different benthic materials. This assessment of image suitability can be performed without field data collection and may therefore aid in screening suitable image datasets.

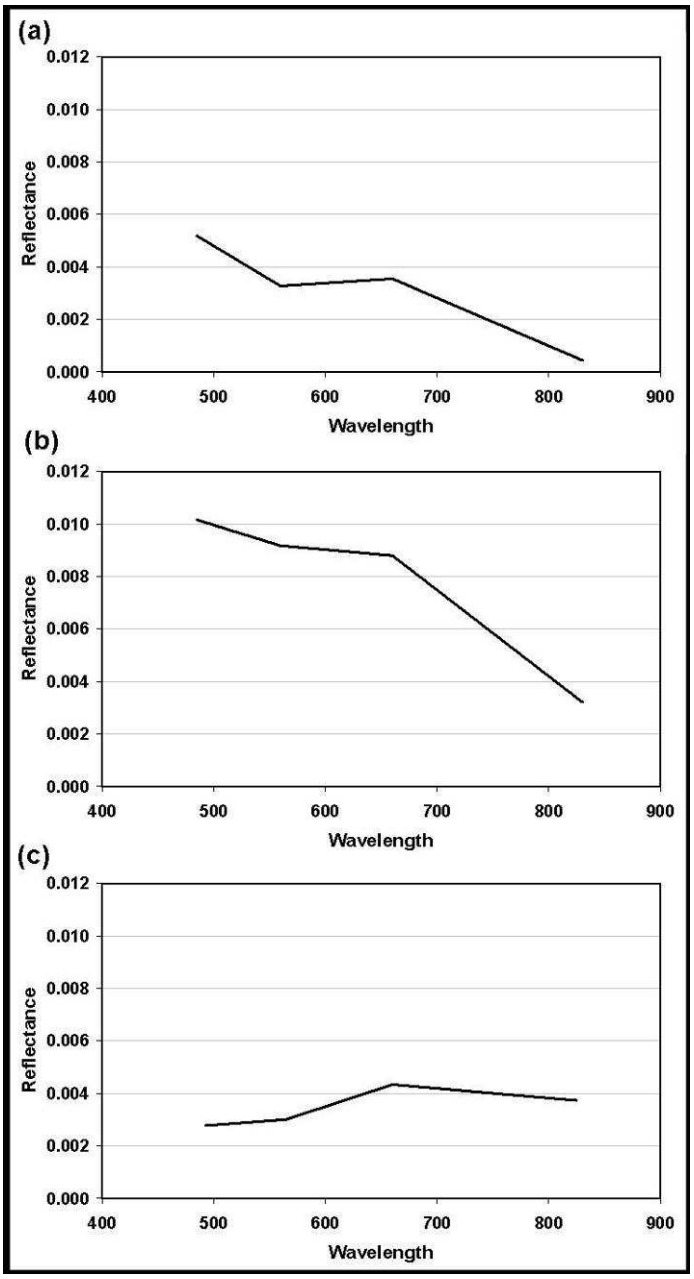

Figure 11 The environmental noise equivalent (NE∆R0-) spectra for each band in (a) the Red Rocks point Quickbird image, (b) the Broke Inlet QuickBird image and (c) the Landsat 7ETM+ image acquired on 03/03/2000. A value of 0.004 means that it is impossible to discriminate any signal difference smaller than 0.4 % reflectance.

Data volume reduction

In order to reduce the processing time of the computationally intensive inverted physics-based radiative transfer model, a data volume reduction protocol was implemented. In essence, it groups the image data into a set of spectrally distinct classes. The strength of this approach lies in the use of the in NE∆*R0-* characteristics inherent to the data. The rationale behind this is

straightforward: if two spectra differ by less than the noise levels in the data, they can be grouped as one class with a relatively minimal loss of information.

The advantage of grouping pixels into distinct classes is that each class (which can contain a large number of pixels) is represented by one spectrum, which can be ingested by SAMBUCA. The SAMBUCA output (e.g. water column depth) for each class can then be mapped back to every pixel labelled as pertaining to that class.

3.5 Retrieval of bathymetry, substratum composition and the optically active constituents

The fifth and pivotal step of the integrated physics based mapping approach is a physics based retrieval of bathymetry, substratum composition (i.e. fractional cover of sand, seagrass and macro-algae) from the *R0-* imagery. To this aim, the inversion/optimization method by Lee et al. (1999; 2001; 1998) was enhanced in order to:

1) retrieve the concentrations of optically active constituents in the water column (chlorophyll-a, CDOM and NAP),

2) account for more than one substratum cover type and

3) to estimate the contribution of the substratum to the remote sensing signal. This implementation (in IDL programming language), called SAMBUCA (the Semi-Analytical Model for Bathymetry, Un-mixing, and Concentration Assessment), is available from the authors upon request.

Principles of the physics based method

At the core of the inversion/optimization method by Lee et al. (1999; 2001; 1998) lies an analytical expression for *R0-* for an optical shallow water body (Maritorena et al. 1994):

$$R_{0-} = R_{0-}^{dp} + \exp(-K_d H)[A\exp(-\kappa_B H) - R_{0-}^{dp}\exp(-\kappa_C H)] \quad (6)$$

where, R_{0-}^{dp} is subsurface remote-sensing reflectance over a hypothetical optically deep water column; H is the water depth; A the bottom albedo (substratum reflectance); K_d *the* vertical attenuation coefficient for diffuse downwelling light, κ_B the vertical attenuation coefficient for diffuse upwelling light originating from the bottom; and κ_C the vertical attenuation coefficient for diffuse upwelling light originating from each layer in the water column. Note that the attenuation of the upward flux is not equivalent to the attenuation of the downward flux (K_d). Attenuation of the upward flux must further be separated into a component originating from the water column (κ_C) and that originating from the bottom (κ_B) (Maritorena et al. 1994). By relating the four quantities R_{0-}^{dp}, K_d, κ_B and κ_C to absorption and backscattering via a series of semi-analytical relationships, Lee et al. (1999; 2001; 1998) modelled the R(0-) spectrum as a function of five independent variables (representing properties of water column and bottom):

$R0- = f(P, G, X, B, H)$ (7)

where P, G, X, and B are scalar values and represent absorption coefficients of phytoplankton and gelbstoff (coloured dissolved organic matter plus detritus), backscattering coefficient of suspended particles, and bottom reflectance at a reference wavelength, respectively; and H is the bottom depth.

3.5.1 Semi Analytical Model for Bathymetry Unmixing and Concentration Assessment (SAMBUCA)

In the inversion-optimization scheme in SAMBUCA the modelled subsurface remote-sensing reflectance ($R0-^{model}$) is compared to the measured subsurface remote-sensing reflectance ($R0-^{input}$) which was obtained from each pixel in the remote sensing image. The set of variables that minimises the difference between these two spectra is used to estimate the environmental variables being sought, e.g. water column depth, substratum composition or the concentrations of the optically active constituents of the water column.

The extraction of environmental information from measured reflectance spectra constitutes a radiative transfer inverse problem. Inverse problems are notoriously difficult because of potential non-uniqueness issues (Mobley et al. 2005). It is often necessary to constrain inverse problems so as to guide the inversion to the correct solution. Such constraints often take the form of simplifying assumptions about the underlying physical or mathematical problem, or of added environmental information. For the inversion-optimization in SAMBUCA, the Downhill Simplex method was adopted, whilst ranges for variables to be optimized were constrained to reduce the occurrence of spectral ambiguities (Wettle and Brando 2006; Wettle et al. 2005).

In SAMBUCA, the algorithm by Lee et al. (1999; 2001; 1998) was modified to retrieve the concentrations of optically active constituents in the water column (chlorophyll-a, CDOM and NAP). The absorption and backscattering coefficients are described as the sum of the contributions of N constituents and a constant coefficient for pure water:

$$a = a_w + \sum_{j=1}^{N} a_j^* C_j \;;\; b_b = b_{bw} + \sum_{j=1}^{N} b_{bj}^* C_j \quad (8)$$

Where a_w and b_{bw} are the absorption and backscattering of pure water (Morel 1974; Pope and Fry 1997), a_j^* and b_{bj}^* are the specific inherent optical properties (SIOPs) of j^{th} constituent with concentration C_j. In the formulation of equation (8) CDOM has no backscattering term associated with it, and $a^*_{CDOM}(440nm)$represents the concentration of CDOM.

The non-water absorption terms are parameterized as a known shape with an unknown magnitude:

$$a_{phy}(\lambda) = C_{CHL} \cdot a^*_{phy}(\lambda) \quad (9)$$

$$a_{CDOM}(\lambda) = C_{CDOM} \cdot a^*_{CDOM}(\lambda_0) \exp\left[-S_{CDOM}(\lambda - \lambda_0)\right] \quad (10)$$

$$a_{\mathrm{NAP}}(\lambda) = C_{NAP} \cdot a^{*}_{\mathrm{NAP}}(\lambda_0)\exp\left[-S_{\mathrm{NAP}}(\lambda-\lambda_0)\right] \quad (11)$$

Where C_{CHL} is the concentration of chlorophyll-a and $a^*_{phy}(\lambda)$is the chlorophyll-a specific absorption spectrum. As the concentration of CDOM (C_{CDOM}) is represented by $a^*_{CDOM}(440nm)$, the reference wavelength λ_0 was set at 440 nm, S_{CDOM} is the spectral decay constant for CDOM absorption coefficient and $a^*_{CDOM}(\lambda_0)$is set to 1. C_{NAP} is the concentration of NAP; $a^*_{NAP}(\lambda_0)$is the specific absorption of NAP at the reference wavelength, and S_{NAP} is the spectral slope constant for NAP absorption coefficient; and the reference wavelength λ_0 was set at 440 nm for the NAP absorption coefficient.

The non-water backscattering terms are parameterized as follows:

$$b_{bp} = b_{bphy} + b_{bNAP} \quad (12)$$

$$b_{bphy}(\lambda) = C_{CHL} \cdot b^{*}_{bphy}(\lambda_0)\left(\frac{\lambda_0}{\lambda}\right)^{Y_{phy}} \quad (13)$$

$$b_{b\mathrm{NAP}}(\lambda) = C_{NAP} \cdot b^{*}_{b\mathrm{NAP}}(\lambda_0)\left(\frac{\lambda_0}{\lambda}\right)^{Y_{\mathrm{NAP}}} \quad (14)$$

where $b^*_{bphy}(\lambda_0)$ is the specific backscattering of algal particles at the reference wavelength, Y_{phy} the power law exponent for the algal particles coefficient; $b^*_{NAP}(\lambda_0)$ is the specific backscattering of NAP at the reference wavelength, Y_{NAP} the power law exponent for NAP backscattering coefficient. The reference wavelength λ_0 was set at 542 nm for both algal and non algal particle backscattering coefficient.

In SAMBUCA, the algorithm by Lee et al. (1999; 2001; 1998) was modified to account for more than one substratum cover type in a pixel or spectrum by expressing the bottom albedo $A(\lambda)$ (or bottom reflectance) as a linear combination of two substrata:

$$A(\lambda) = q_{ij}A_i(\lambda) + (1-q_{ij})A(\lambda) \quad (15)$$

Where q_{ij} represents the fractional cover of substratum i and substratum j within each pixel, $A_i(\lambda)$ and $A_j(\lambda)$ are the albedos of substratum i and j, respectively. When solving for more that two cover types, SAMBUCA cycles through a given spectral library, retaining those two substrata and their estimated fractional cover q_{ij} which achieve the best spectral fit.

In summary, the complete model parameterization of equation (8) for SAMBUCA is:

$$r_{rs}^{\mathrm{model}} = f\begin{pmatrix} C_{CHL}, C_{CDOM}, C_{NAP}, H, q_{ij}, A_i(\lambda), A_j(\lambda), S_{CDOM}, S_{NAP}, \\ Y_{PHY}, Y_{NAP}, a^{*}_{\mathrm{PHY}}(\lambda), a^{*}_{\mathrm{NAP}}(\lambda_0), b^{*}_{b\mathrm{PHY}}(\lambda_0), b^{*}_{b\mathrm{NAP}}(\lambda_0) \end{pmatrix} \quad (16)$$

Optical properties of benthic substrates

The benthic substrate parameterization used in this project was based on three substrate types: sand, macro algae and seagrass. The reflectance spectra used to represent these substrate types (Figure 12) are taken from a substrate spectral library collected at Fish Creek and Two Peoples Bay during the November 2008 field campaign.

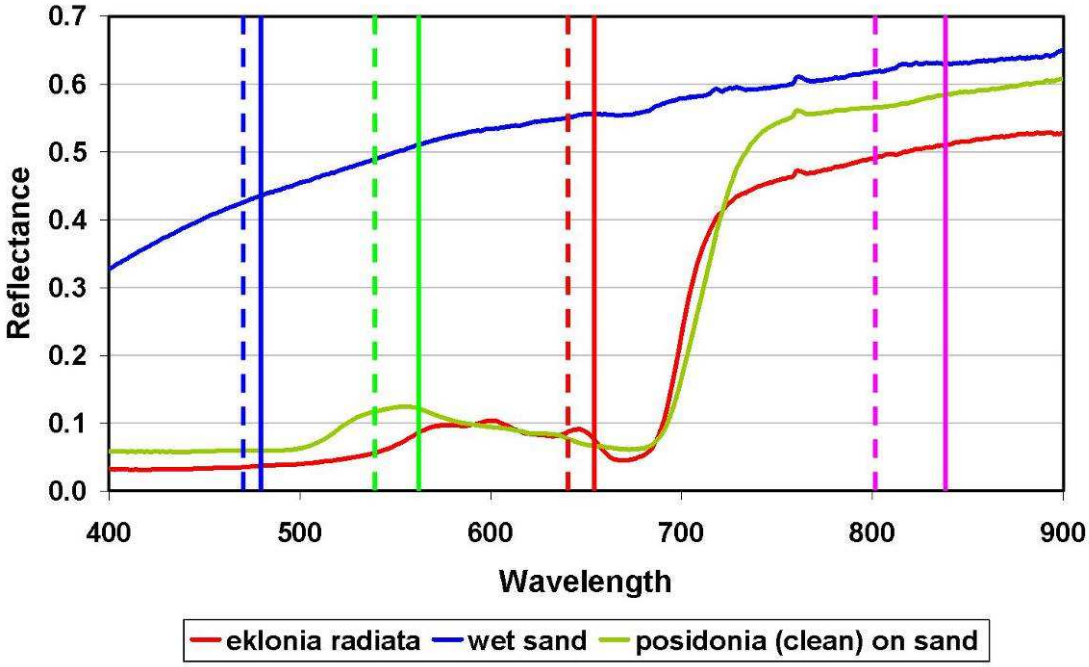

Figure 12 Reflectance spectra of macro algae, sand and seagrass used to define the benthic substrate parameterization within SAMBUCA. The solid blue, green, red and magenta lines show the central wavelength location of the Landsat blue, green, red and NIR channels while the corresponding dotted lines show the location of the QuickBird blue, green red and NIR channels. The human eye can see from the blue at about 400 nm to the red at about 690 nm.

Optical properties of WA coastal waters

The parameterisation of the semi-analytical model (eq. 16) relies on field sampling of the optical properties of the water body of interest. When this is not possible, the semi-analytical model (eq. 16) can be parameterized with sites of similar characteristics from the literature. For this project, inherent and apparent optical properties of the study sites were not measured. The optical parameterization of water defined for SAMBUCA in this project was based on a comprehensive field campaign at Cockburn Sound, WA in 2003 (Table 4 and Figure 13) as this was deemed the most closely related water column property data from all of CSIRO's spectral measurements. A dedicated sampling and optical property analysis is recommended for these SW Australian waters to confirm this choice of parameterisation.

Table 4 Optical domain, based on samples collected by CSIRO at Cockburn Sound in 2003, of WA coastal waters as defined for SAMBUCA

	Parameter values
C_{CHL} (µg/L)	1.2
C_{TR} (mg/L)	0.7 - 3.6 (range)
C_{CDOM} (conc)	0.01
S_C	0.0106
S_{TR}	0.0106
a^*_{TR} (550)	0.0154
X_{PHY}	0.00033
X_{TR}	0.0047
aphy*	See Figure 13
Y	0.717

Where

C_{CHL} = concentration of chlorophyll a

C_{CDOM} = concentration of CDOM where a*CDOM (550) is set to 1

S_C = slope of CDOM absorption

C_{TR} = concentration of NAP (tripton)

S_{TR} = slope of NAP (tripton) absorption

a*TR (550) = specific absorption of NAP (tripton) at 550nm

X_{PHY} = specific backscattering due to phytoplankton

X_{TR} = specific backscattering due to NAP (tripton)

aphy* = specific absorption of chlorophyll, as shown in Figure 13

Y = slope of the particulate (phytoplankton or tripton) backscattering

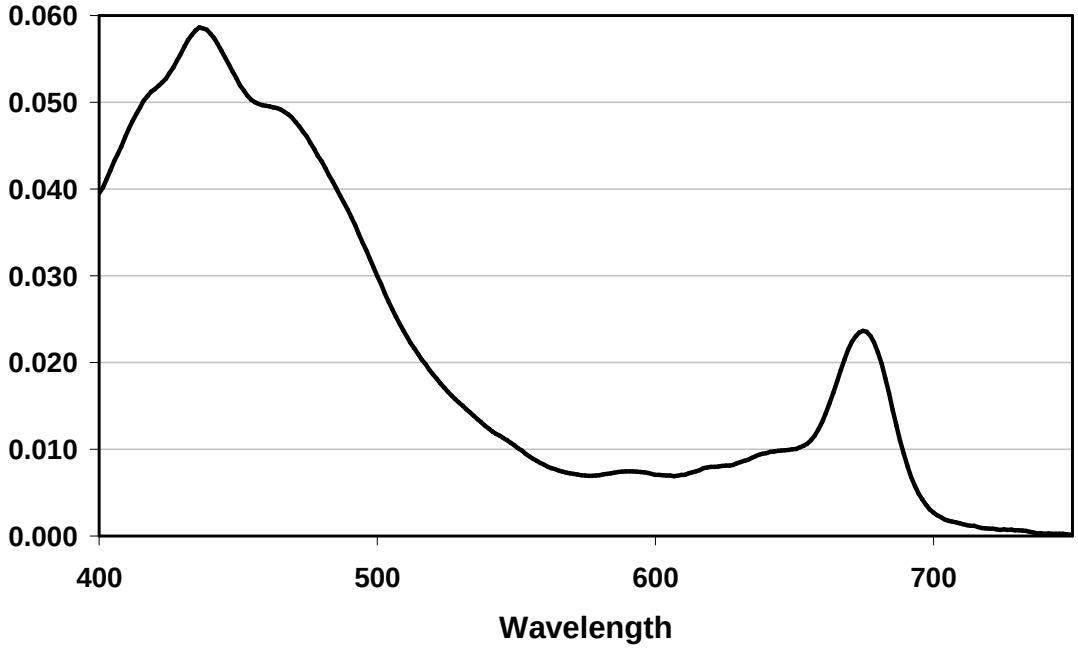

Figure 13 Specific absorption of phytoplankton (m^2mg^{-1}) as measured for Cockburn Sound water samples and used in the parameterization of SAMBUCA for WA south coast waters (Table 4). Note the two major chlorophyll a light absorption features at 438 nm and at 676 nm.

Based on the parameterization, SAMBUCA was configured to estimate the concentrations of optically active constituents in the water column (chlorophyll-a, CDOM and NAP), water column depth, and benthic substratum composition that produces the best fit between modelled and measured R(0-) on a pixel-by-pixel basis.

4. RESULTS

The ideal mechanism for evaluating the success of the model substratum retrieval is to compare the bathymetry output to known field measurements. These were not available during the execution of this work, thus error analysis had to be based on the spectral closure achieved by SAMBUCA. It is recommended to collate a dataset of known depths from either ship-based measurements or from aircraft (using e.g. the Laser Airborne Depth Sounder-LADS). A minimum of ten to twenty points uniformly distributed across a depth range in an image is sufficient.

SAMBUCA uses an optimisation algorithm to simulate the image data R(0-) spectrum as closely as possible. The spectral matching, resulting in a spectral closure, is driven by a function of the difference between the image R(0-) and SAMBUCA R(0-). This variable, αf, is a function of the shape and magnitude of the output spectra, and is retained by SAMBUCA for every estimate. It can therefore be output in map form, and is an indication of the reliability of the SAMBUCA depth estimate. A lower value indicates a better goodness-of-fit, and higher confidence in the retrieval. A more detailed description of the data retrieval and error assessment procedure used in the SAMBUCA model can be found in (Brando et al. 2009)

4.1 Broke Inlet QuickBird

Figure 14 illustrates the difference between the image R(0-) (Figure 14a) and SAMBUCA R(0-) (figure 14b) of the Broke Inlet QuickBird scene. As expected, SAMBUCA achieves a relatively better spectral closure for shallower waters (figure 15), especially where the substratum presents a bright target, such as over sandy patches and light limestone pavement. Here, the substratum contributes more to the measured R(0-) signal, and the magnitude of the signal is higher. This could also be an indication that the parameterisation of the optical properties of the water column may not be representative of this area. At deeper depths SAMBUCA mainly uses the optical properties of the water-column to try and achieve spectral closure. Given that a limited amount of fieldwork was done for this project and that assumptions therefore had to be made concerning the water parameterisation, this is plausible. Additional variability in water quality might also have been introduced by plumes of tannin-rich water from the Broke Inlet (see for example Figure 16) which would have changed the optical properties of the water column beyond the standard SIOP parameterization of the model. It is impossible to gauge from this image whether the water around Broke Inlet was affected by such an outflow at the time when the image was acquired.

It is also apparent that areas that are affected with residual glint also resulted in larger differences between measured and modelled image spectra. This resulted in higher imagery reflectance in the glint-affected pixels which was interpreted by the model as either very shallow water with a bright substratum (Figures 17 and 18) or as a deeper, more turbid, water column.

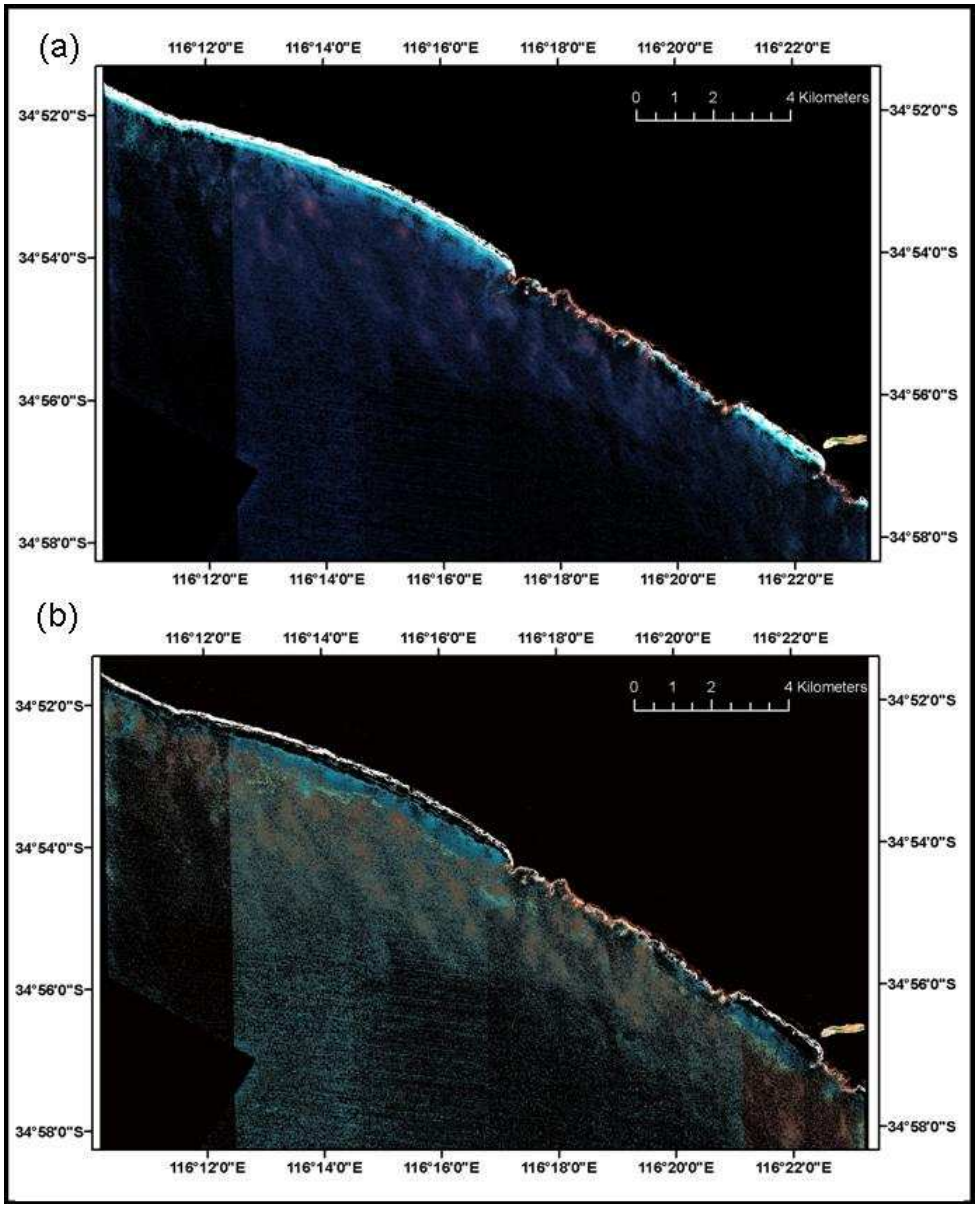

Figure 14 True colour R0- image of Broke Inlet from (a) the atmospherically corrected and land+glint masked QuickBird image and (b) the corresponding spectra as simulated by SAMBUCA. The vertical banding is caused by the 6 CCD's (Charge Coupled Devices) in the QuickBird sensor not being uniformly calibrated over dark water targets. It is recommended to trial an image correction procedure that could remove some of this vertical banding caused by uniformity inconsistencies over dark aquatic targets.

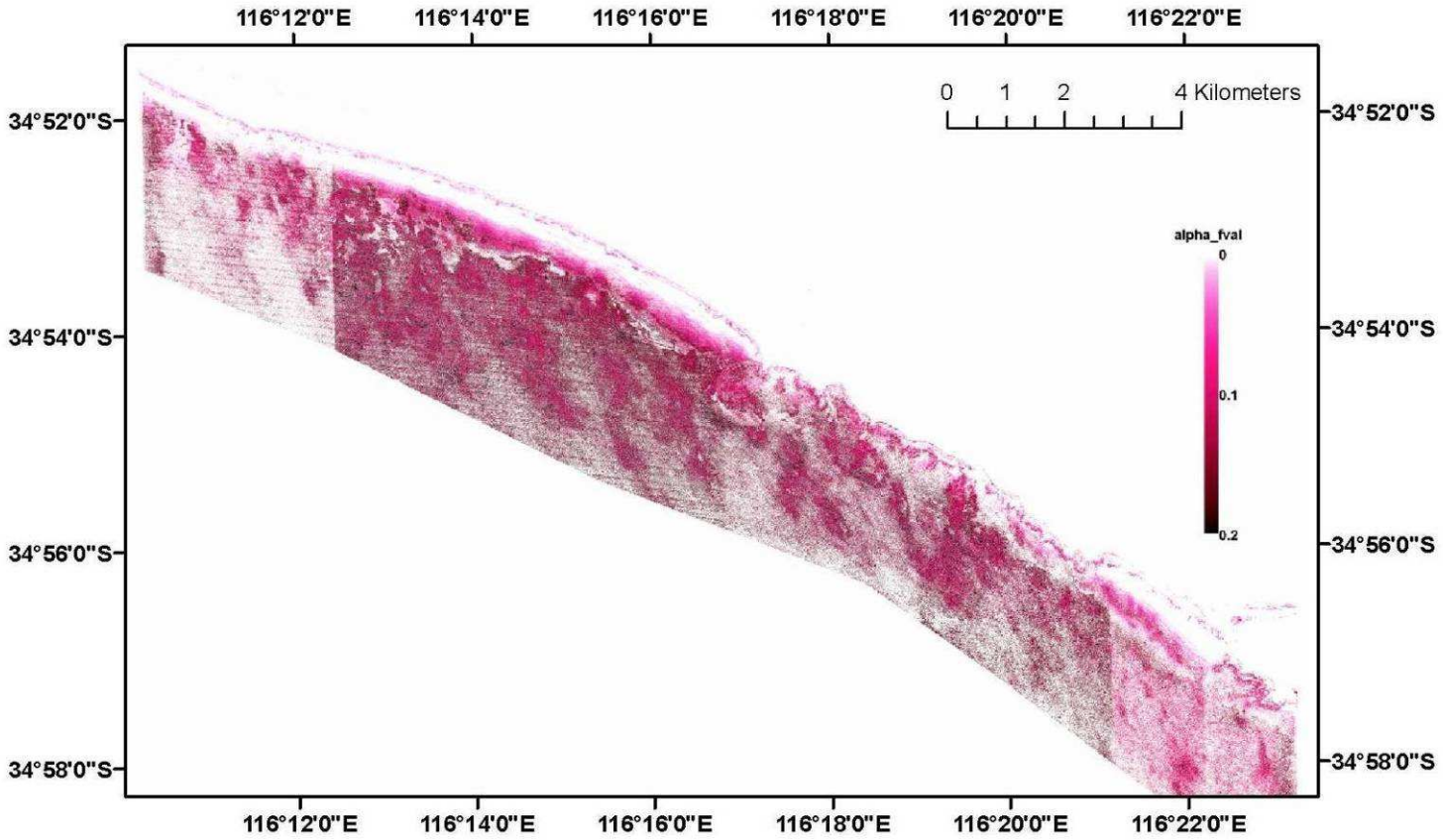

Figure 15 Alpha_fval (αf) as output from SAMBUCA for the Broke Inlet QuickBird scene. Lower values indicate a better fit and, therefore, a theoretically more reliable SAMBUCA benthic cover estimate.

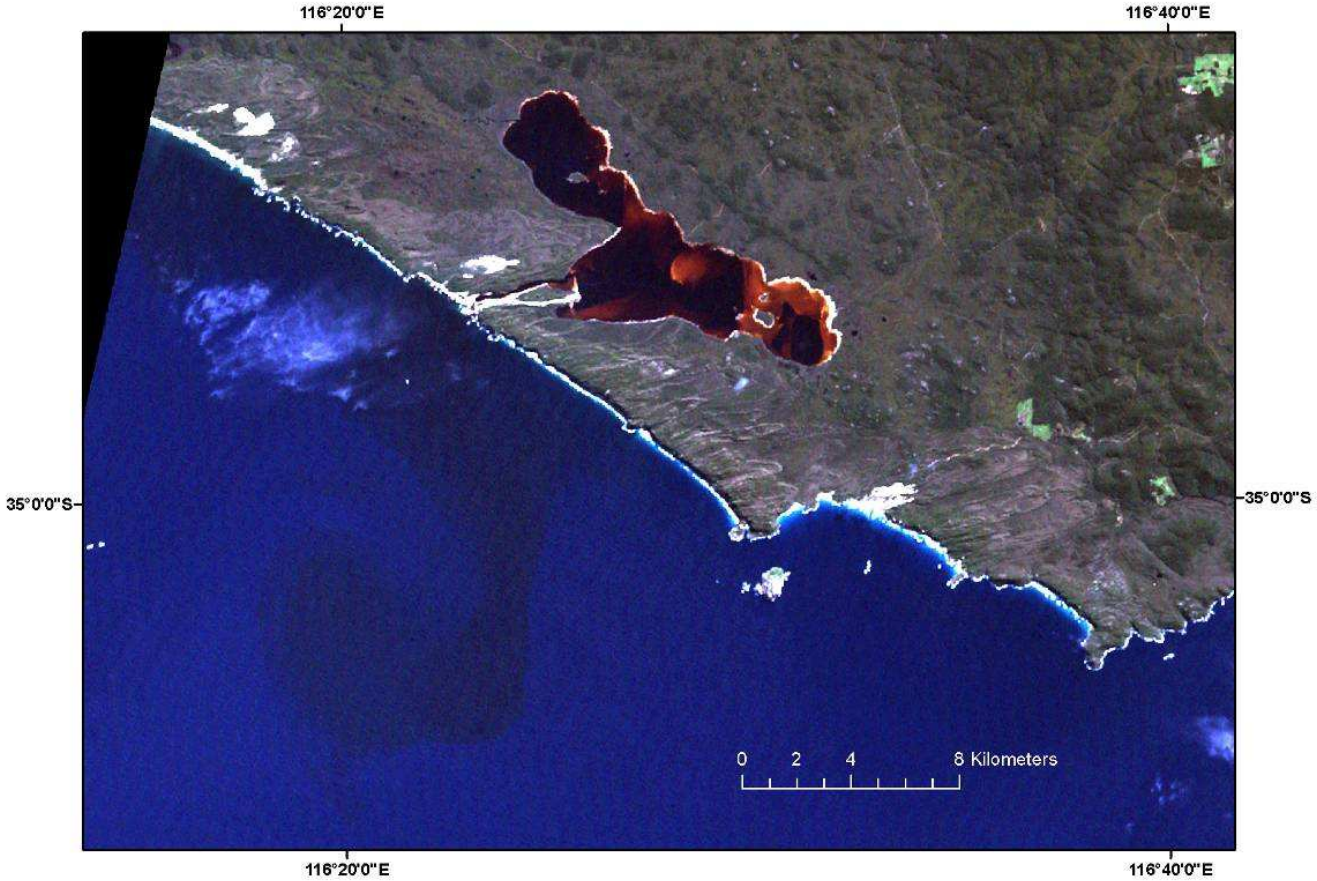

Figure 16 Subset of a Landsat 7 ETM+ image, acquired on 14/08/1999, showing a plume of tannin-rich water flowing up to 14 km from the coast, from the open entrance of the Broke Inlet coastal lake.

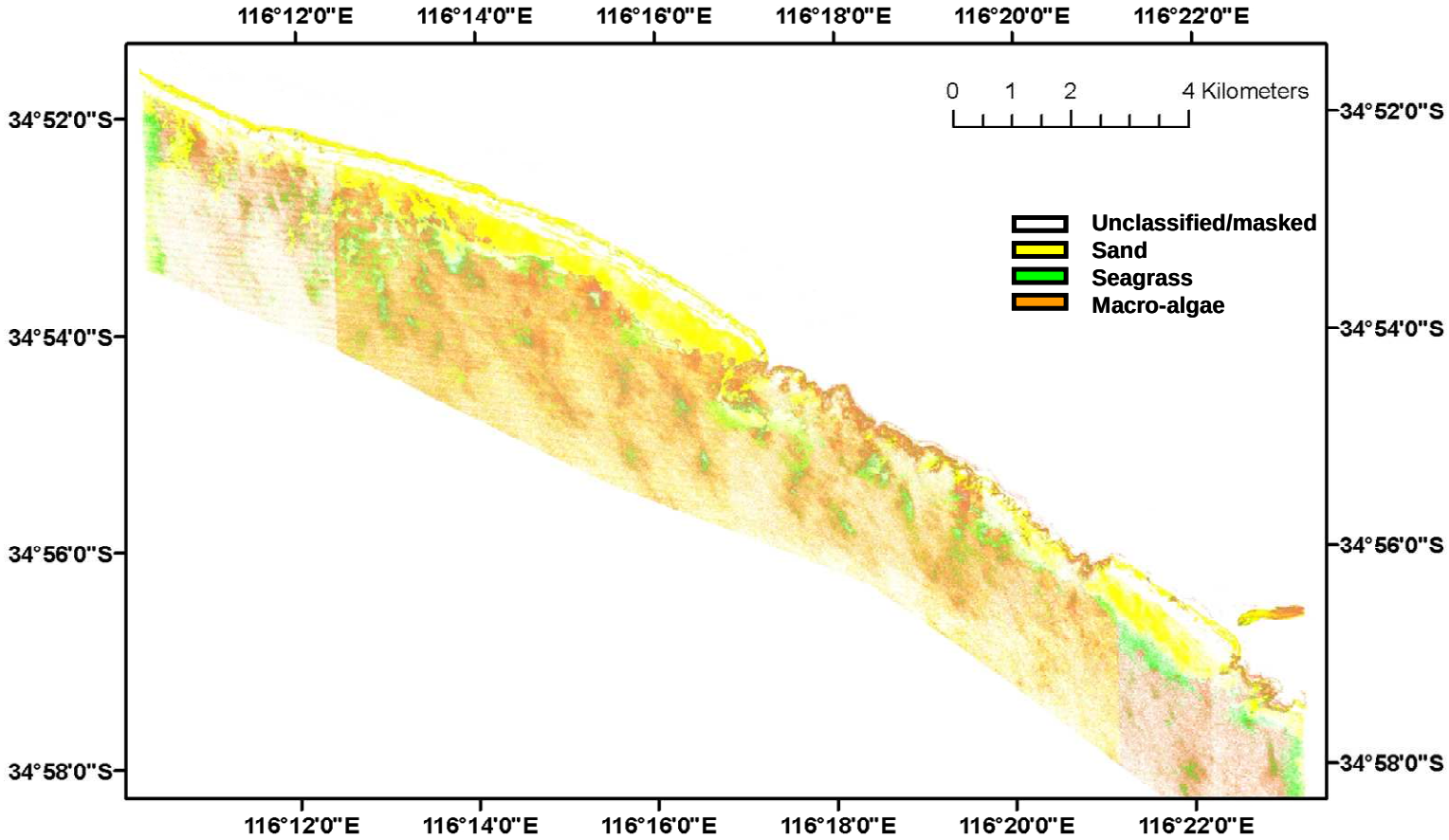

Figure 17 Broke Inlet dominant benthic cover type classification, based on a SAMBUCA model inversion with three possible substrates. Grey represents areas that were masked out either initially due to high glint contamination or post-processing due to bad spectral closure (high αf values).

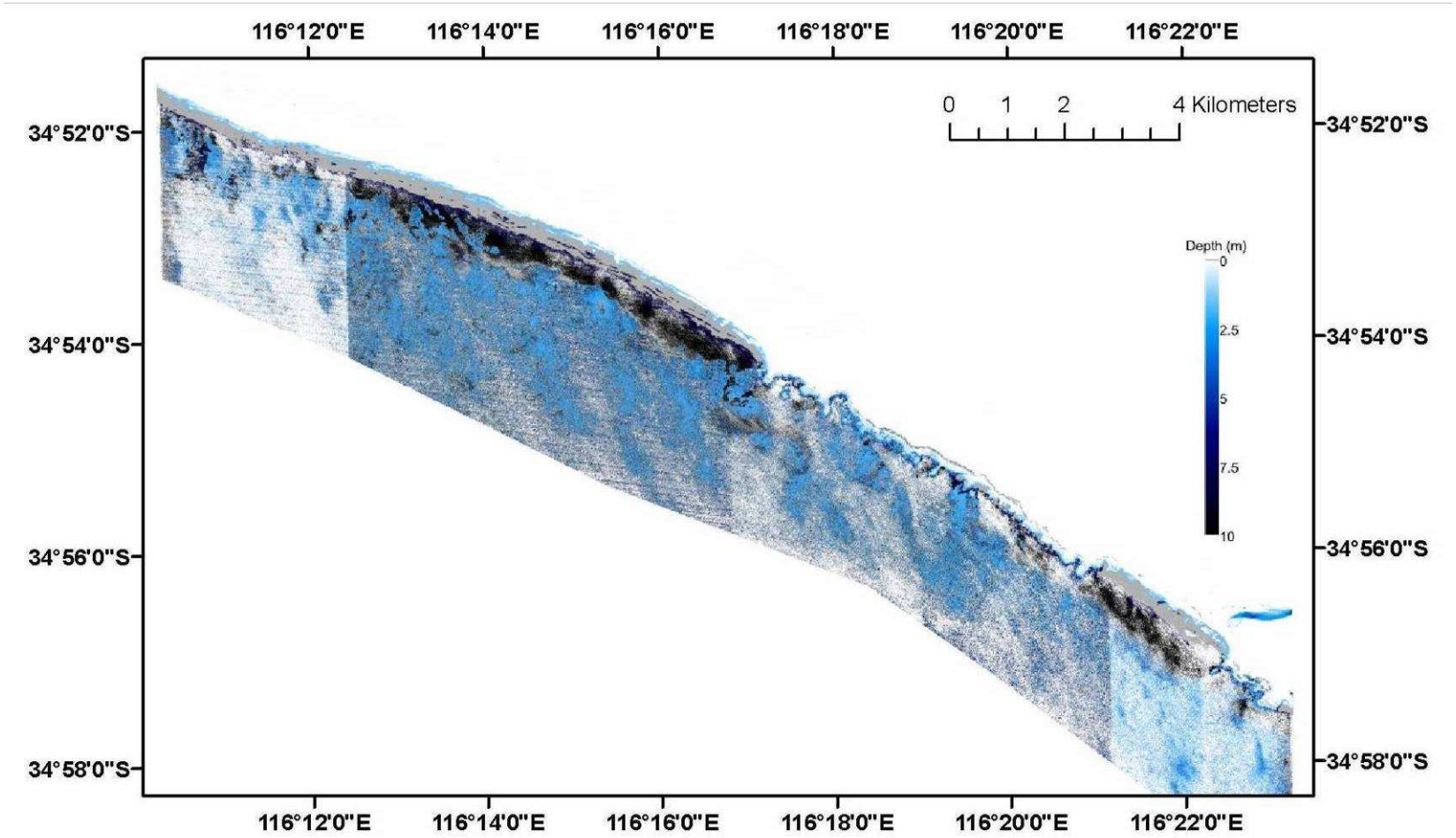

Figure 18 Quality-assessed SAMBUCA bathymetry output from the Broke Inlet QuickBird scene. White and gray represents areas that were masked out either initially due to high glint contamination or post-processing due to bad spectral closure (high αf values) . The 10 m deep values near the surf zone may be artefacts due to inadequate knowledge of the sand spectrum or they could also be deep gutters near the coast.

4.2 Red Rocks Point QuickBird

Figure 19 illustrates the difference between the image R(0-) (Figure 19a) and the simulated SAMBUCA R(0-) (figure 19b) of the Red Rocks Point QuickBird scene. As expected, SAMBUCA achieves a relatively better spectral closure for shallower waters, especially where the substratum appears bright, such as over sandy patches (Figure 20). Here, the substrate contributes more to the measured R(0-) signal, and the magnitude of the signal is higher. This could also be an indication that the parameterisation within SAMBUCA of the optical properties of the water column is not representative of the area. At deeper depths SAMBUCA mainly uses the optical properties of the water-column to try and achieve spectral closure. Given that no fieldwork was done for this project and that assumptions therefore had to be made concerning the water parameterisation, this is plausible.

The vegetated areas in the Red Rocks Point QuickBird image were not modelled very well with SAMBUCA (Figure 19b). These target areas were very dark which resulted in inaccurate model output as the spectral library (collected at Two Peoples Bay and Broke Inlet), was much brighter than much of the vegetated spectra observed in the image. This discrepancy was probably due to the fact that the spectral library was collected from a stack of flattened leaves, presenting a brighter target than upright leaves in water. Target variability is clearly demonstrated in Figure 21, showing the effect of current action on the intensity of light reflected from the individual blades of seagrass. In very dense meadows, less light will be reflected due to the canopy structure causing internal shading and therefore lowering the albedo of the target. Subsequently only very shallow water and sandy patches (Figures 22 and 23) was mapped with any degree of certainty with the physics-based approach used.

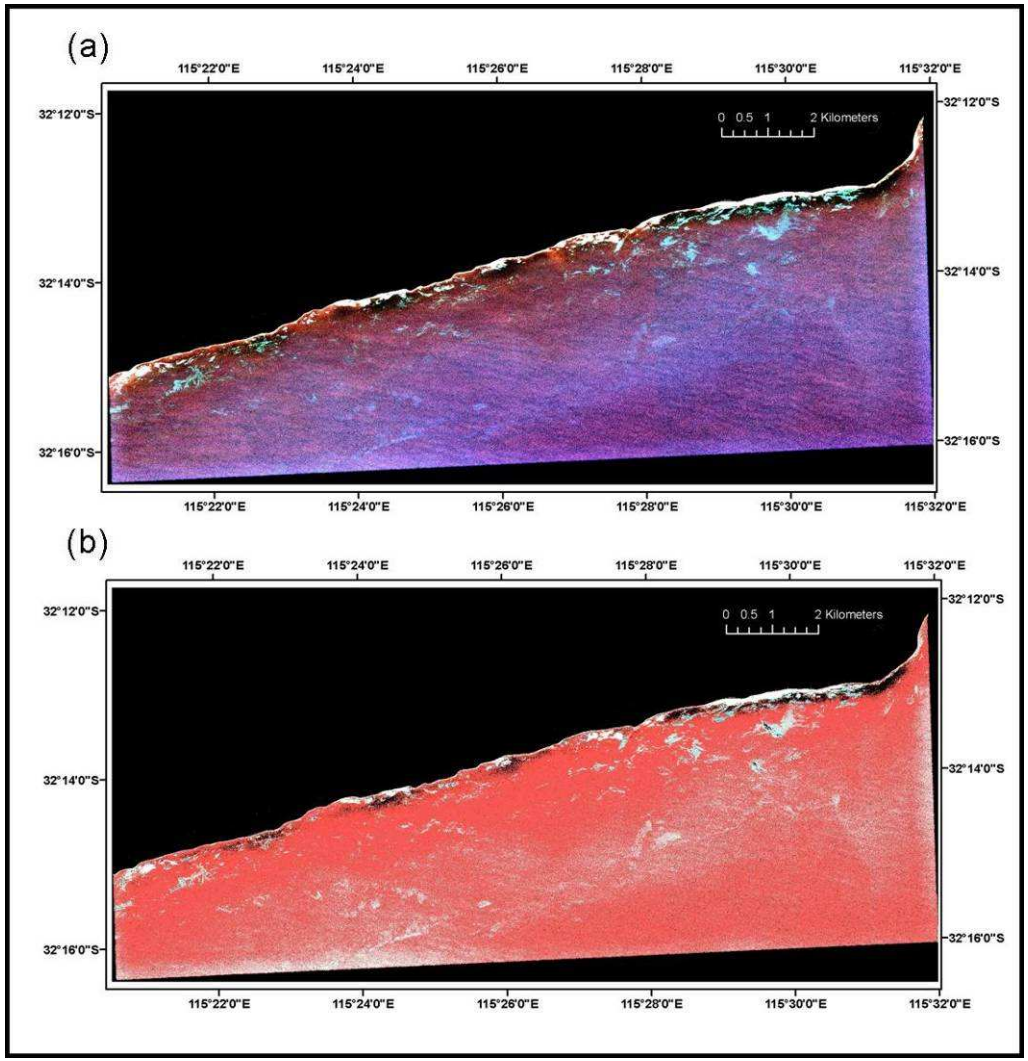

Figure 19 True colour R0- image of Red Rocks Point from (a) the atmospherically corrected and land masked QuickBird image and (b) the corresponding spectra as simulated by SAMBUCA

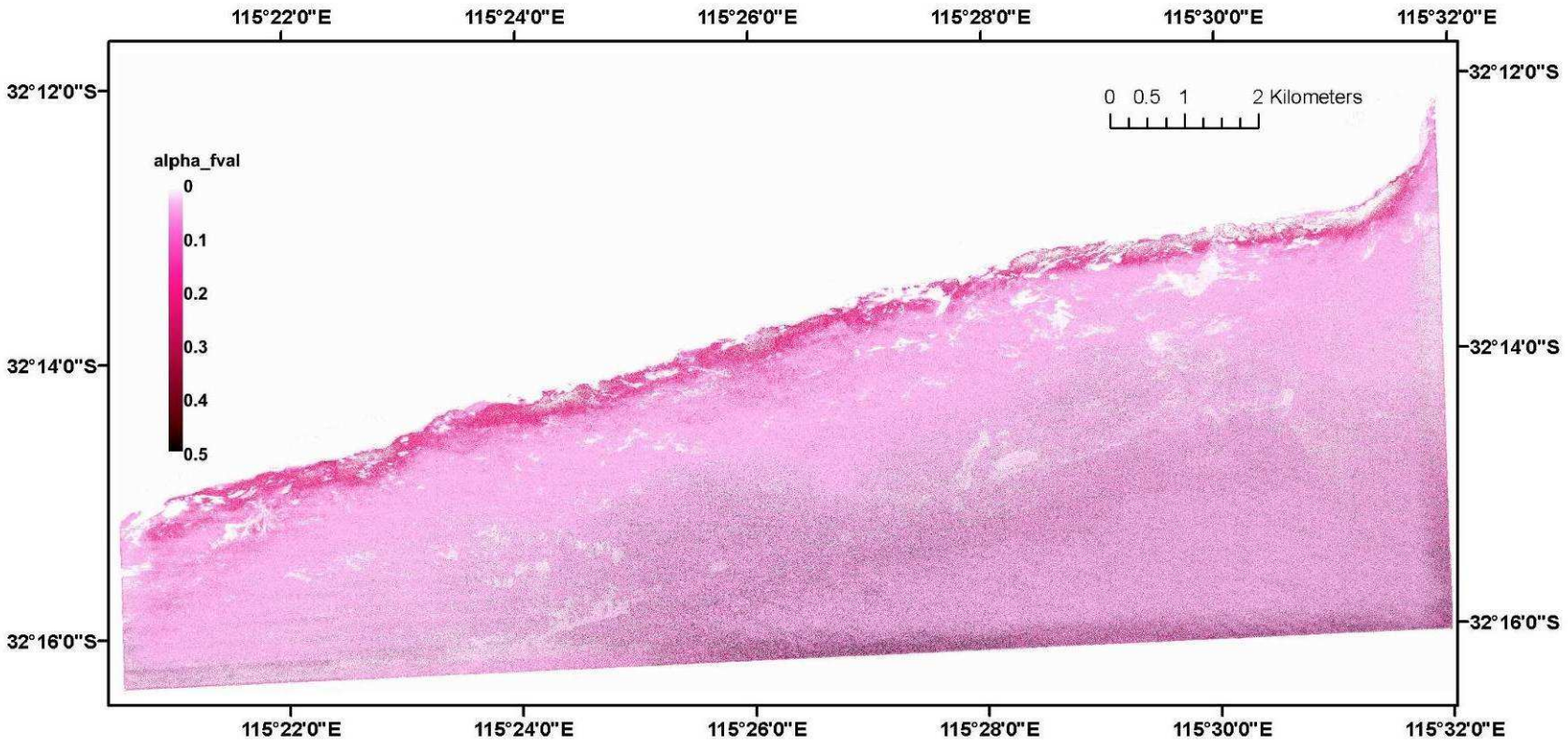

Figure 20 Alpha_fval (αf) as output from SAMBUCA for the Red Rocks Point QuickBird scene. Lower values indicate a better fit and, therefore, a theoretically more reliable SAMBUCA benthic cover estimate

Figure 21 *In situ* photograph of seagrass, taken in Two Peoples Bay, demonstrating the variable response of light to different blade orientations. Despite similar densities, the seagrass at the centre of the image appears darker due to its upright orientation presenting a much smaller target for light to be reflected off than the blades towards the outside of the image which is flattened by wave-action. This can result in significant target variability, especially in dense seagrass or macro algae meadows which can potentially cause estimation errors when using a spectral library of seagrass or macro-algae that was collected from a stack of flattened leaves, resulting in a very bright reflectance target.

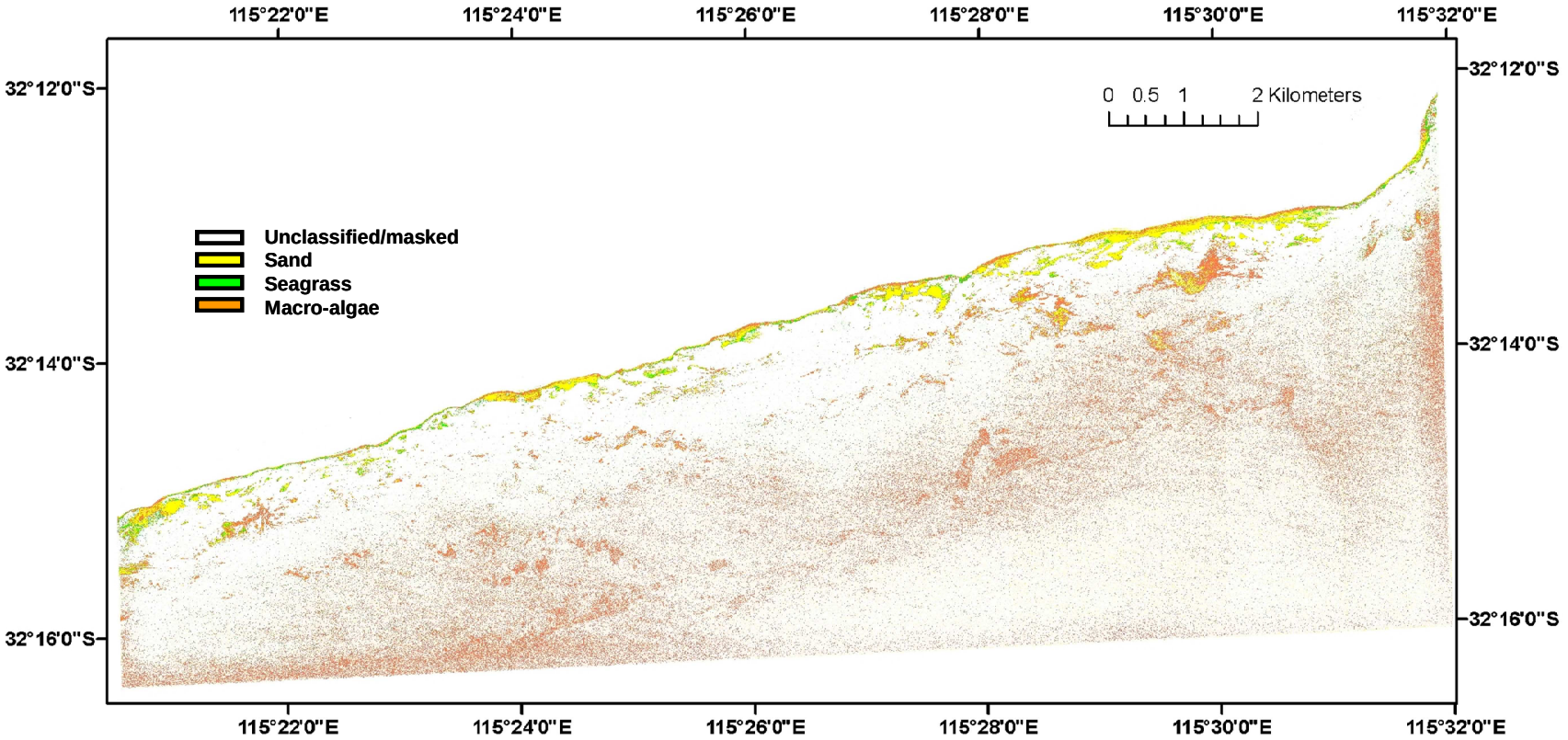

Figure 22 Red Rocks Point dominant benthic cover type classification, based on a SAMBUCA model inversion with three possible substrates. White represents areas that were masked out post-processing due to bad spectral closure

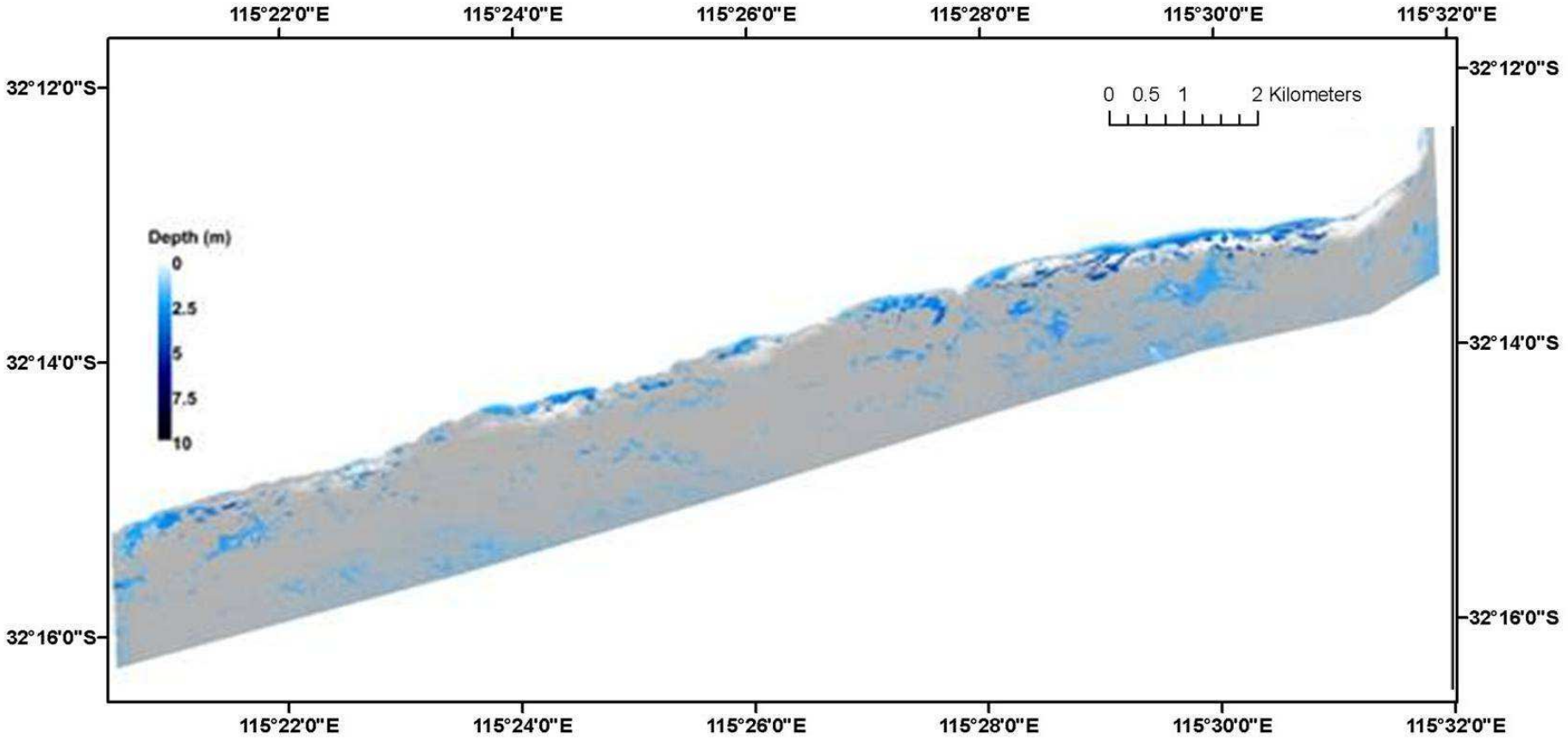

Figure 23 Quality-assessed SAMBUCA bathymetry output from the Red Rocks Point QuickBird scene. White represents areas that were masked out post-processing due to bad spectral closure (high αf values)

4.3 Broke Inlet to Bald Island Landsat image

Similar to the results from the QuickBird data, SAMBUCA achieved a relatively better spectral closure for shallower water, especially where the substratum appears bright, such as over sandy patches (Figure 24 and 25). This could also be an indication that the parameterisation within SAMBUCA of the optical properties of the water column was not representative of this area: at deeper depths SAMBUCA mainly uses the optical properties of the water-column to try and achieve spectral closure. Given that no fieldwork was done for this project and that assumptions therefore had to be made concerning the water parameterisation, this is plausible. Although severely glint-affected pixels were masked out prior to the modelling step (Figure 24a), residual glint still affected the model output in some of the remaining pixels (Figure 24b). This resulted in higher measured reflectance in the glint-affected pixels which was interpreted by the model as either very shallow water or a bright substratum (Figure 26 and 27).

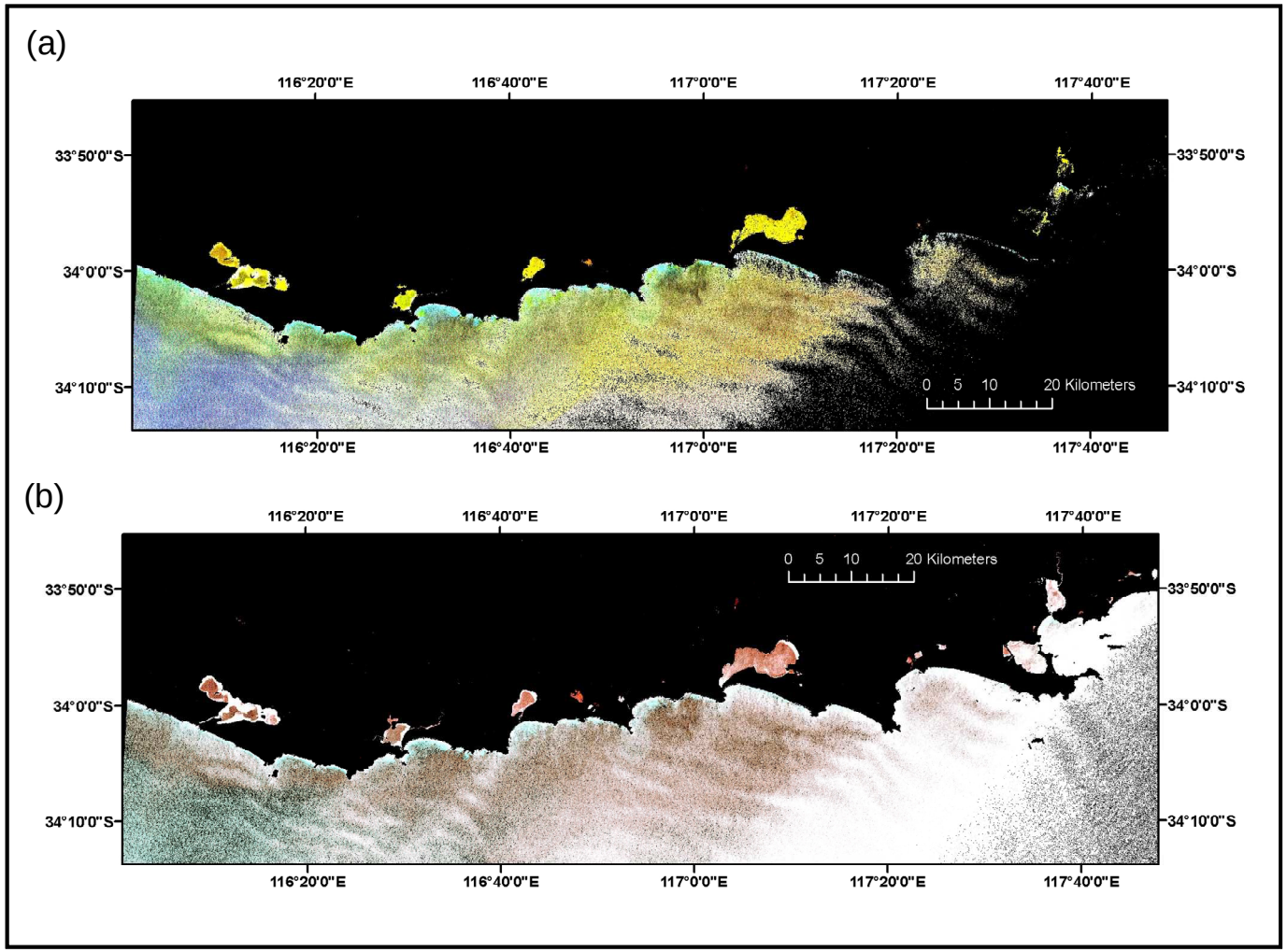

Figure 24 True colour R0- image of the coastline between Broke Inlet to Bald Island from (a) the atmospherically corrected and land masked Landsat 7ETM+ image and (b) the corresponding spectra as simulated by SAMBUCA

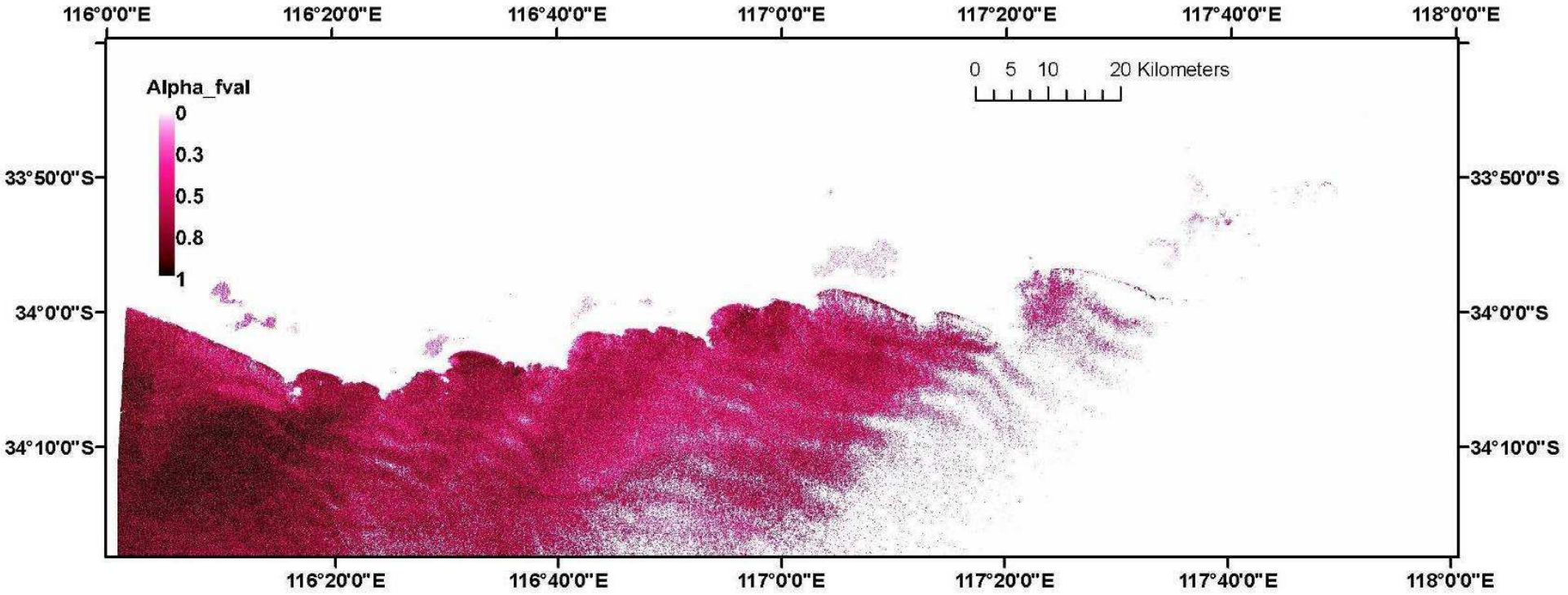

Figure 25 Fval (f) as output from SAMBUCA for the Broke Inlet to Bald Island Landsat scene. Lower values indicate a better fit and, therefore, a theoretically more reliable SAMBUCA benthic cover estimate

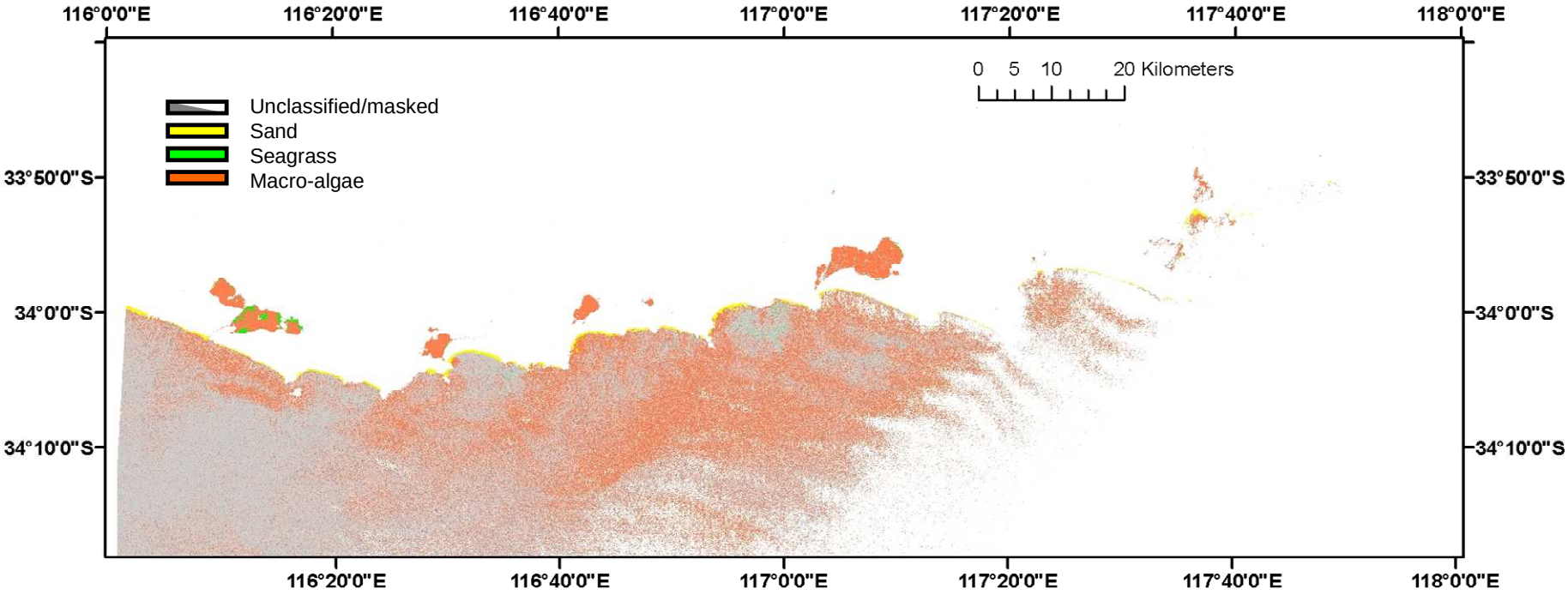

Figure 26 Dominant benthic cover type classification of the section of the WA coast between Broke Inlet and Bald Island, based on a SAMBUCA model inversion with three possible substrates. White and gray represents areas that were masked out pre-processing due to severe sunglint or post-processing due to bad spectral closure.

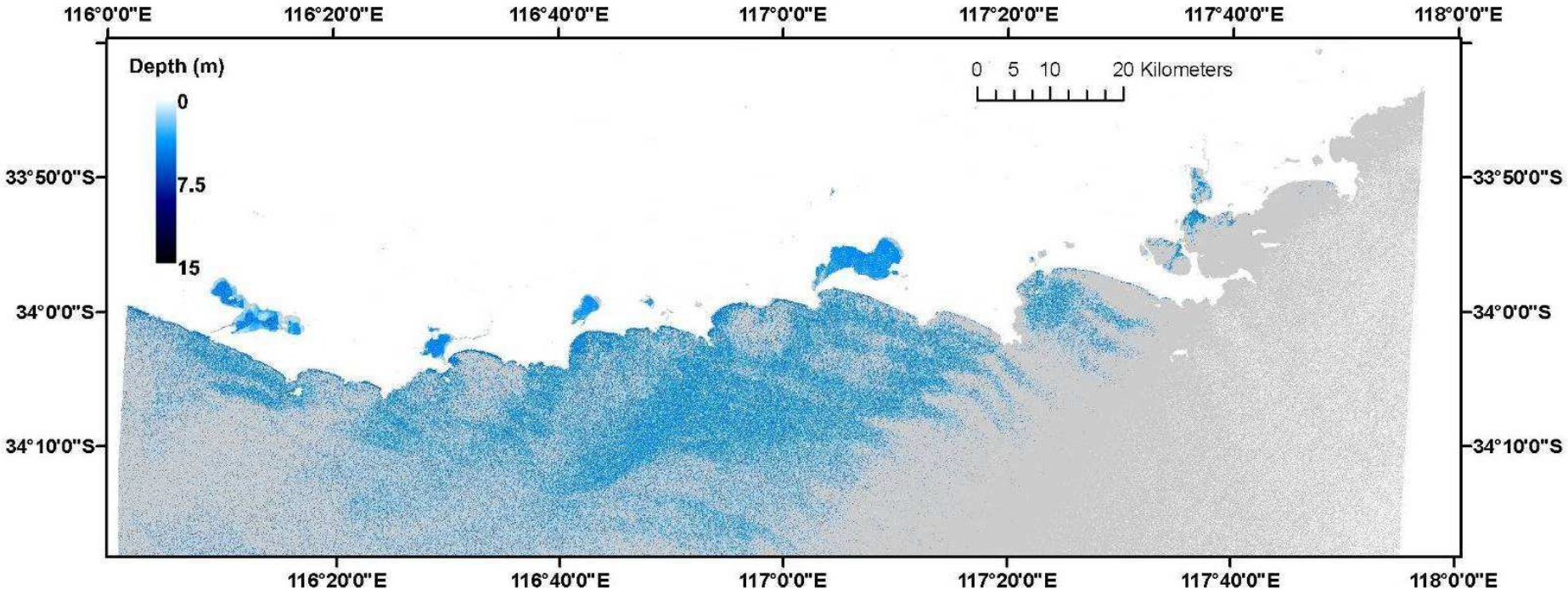

Figure 27 Quality-assessed SAMBUCA bathymetry output from the Broke Inlet to Bald Island Landsat scene. Gray represents areas that were masked out post-processing due to bad spectral closure (high f values)

5. DISCUSSION AND RECOMMENDATIONS

5.1 Discussion

The aim of this project was to demonstrate if and how earth observation from archival image data (from Landsat and QuickBird images) could help in coastal marine benthic habitat mapping of selected poorly documented areas of the SW Australian shallow coastal waters. Due to the preliminary nature of this project, relatively short timelines and funding constraints, no dedicated fieldwork was possible to adequately parameterize the physics-based processing pathway implemented. A short fieldwork was performed for exploratory data collection of *in situ* data only. During the snorkel based sampling in Two Peoples Bay a possible new *Riphillia* species was found. It was selected for spectral measurement due to its deviating colour from surrounding macro-algae and seagrasses.

This feasibility study was a partial success. Keeping in mind this was a relatively short and small project for such a large task, the results are promising. It was feasible to discriminate sandy patches from vegetated areas from each image and it was also feasible to distinguish macro-algae from seagrasses in the shallower areas where there is sufficient signal coming from the substratum (roughly speaking to about 1 or 1.5 km offshore). Due to lack of in situ data no estimate of validity could be made other than that the patterns seem to agree with anecdotal evidence of locally engaged DEC staff. After quality assessment, near-shore bathymetry maps were also produced that may potentially augment existing bathymetry datasets.

In addition to the proposed project deliverables, the Landsat image of August 1999 is a good demonstration of the power of remote sensing to detect short-term environmental events phenomena such as, in this case, the outflow of tannin rich waters in to the coastal water. The plumes apparently do not mix immediately and can be seen to 14 kilometres offshore. Presumably these plumes are buoyant (although some of the lake water may be as saline as or more saline than the ocean waters-on the other hand once these lakes overflow there must be a substantial amount of runoff diluting the saline waters) based upon their consistency to far offshore. The water temperature difference (warmer lake water?) may also cause this effect.

A start has been made with creating a spectral library of substratum type and substratum cover (seagrasses, macro-algae and epiphytes) that will always be useful for future applications in this area. A thematic gap in the availability of South West WA benthic spectral data in the national spectral library has been partially addressed during the short field campaign. This spectral data will be especially useful for implementation with future, more sophisticated, sensors with higher spectral resolution.

To adequately perform coastal change-detection from satellite imagery, images have to be normalized to eliminate the effects of different sun angles, sky glint, water column depth and turbidity as well as atmospheric effects present at the time of image acquisition. The only way

to perform this task adequately is to implement a physics based approach, possibly augmented by object oriented image processing software such as e-Cognition that can take contextual information and pattern and texture information into consideration.

5.1.1 Specific issues that require further work:

Landsat image data

- Sourcing the image data: for a physics-based inversion method (that is the most advisable method for multi-temporal image processing) it is essential that the radiometric data integrity is maintained. As this Landsat image was obtained though Landgate with unknown preprocessing applied, the radiometric data quality was compromised. It is advised to obtain unprocessed imagery in future or alternatively, to obtain exact information on preprocessing applied to back calculate the imagery to preprocessing status.

- Atmospheric correction: The MODTRAN based atmospheric correction protocol used in the physics-based processing pathway was not able to adequately correct the Landsat image. This was due to a suspected green spectral band anomaly possibly caused by Landgate preprocessing. As the satellite image was sourced from Landgate, it was not possible to validate the radiometric calibration implemented on the original image.

- Image quality: Landsat images show serious banding across the image reducing their useability. However the 25 years of archive of Landsat data is of paramount interest to do change detection. More attention to removing these banding effects may improve the data quality. For banding removal the raw uncorrected imagery is required.

QuickBird image data:

- Only in the later stages of this project did the CSIRO team find out there was a quality control issue with the radiometric calibration of the QuickBird sensor. QuickBird image products are optimized for radiometric image quality over terrestrial targets which compromise the radiometric integrity of aquatic targets in some cases, especially in images acquired prior to June 2003. As CSIRO applies a physics based atmospheric and air-water interface correction and processing method this radiometric uncertainty affects the results. CSIRO is currently communicating with Digital Globe engineers to clarify this issue and will spend some time in the near-future researching strategies to improve the processing pathway to deal with this source of error.

The water conditions on the southwest Australian coast:

- Large swell and high waves add considerable noise to the images, decreasing the amount of information to be extracted from the substratum. This actually increases and decreases the water column depth causing high frequency changes to water depth (by definition causing a varying portion of the signal measured in space to be from the water column or from the substratum).

- Waves and swell also causes severe sunglint and skyglint. Although methods do exist to remove part of this effect, total removal is unlikely.

Field radiometry

- The seagrass and macro-algae spectra in the spectral library collected at Broke Inlet and Two Peoples Bay had a much higher albedo than target spectra observed in the QuickBird imagery, especially in the Red Rocks Point image. This suggests that the way the spectra were measured, from flattened leaf blades on the beach, may not be representative of the *in situ* light environment where leaves are floating upright in the water causing significant shading within the canopy thus reducing the albedo.

Depth assessments

- It seemed feasible to get a rough estimate of water column depth. Most images showed that the maximum depth to which substratum could be mapped into coarse categories is about eight meters for these waters under the conditions of the image acquisition

5.2 Recommendations:

5.2.1 Image data quality:

- Provide raw satellite imagery with the radiometric calibration coefficients applied separately to avoid calibration uncertainties and ascertain the radiometric calibration of any remote sensor used prior to purchasing the data.

- One possible way to circumvent the noise due to environmental conditions is to start analysing multiple images of the same area after stripping all doubtful data out of each image and only using the pixels with good data content. As the environmental conditions will occur randomly within an image, this should enable construction of a synthetic best image. Such an approach is especially suitable for estimating water column depth more reliably. Once the water column depth is known this can be input into the inversion algorithm as a known variable thereby allowing the inversion algorithm to increase focus on the substratum composition.

- Consider the use of sensors such as ALOS-AVNIR (10 m pixel resolution) and IKONOS (4 m pixel resolution) and others to increase the choice of images.

- Future sensors will have more spectral bands allowing more discrimination of features at the substratum. For example the WorldView-2 satellite will have finer spatial resolution than QuickBird (at 1.8 m pixels) with eight instead of four spectral bands thus doubling the amount of spectral information.

- It is also recommended to study the climatology of this coast to find the seasonal optimal times for calmer waters as well as the optimal times that avoid sun glint occurring as much as possible.

- Acquiring image data at lowest low tide may also be an option for obtaining imagery with as much bottom information as possible.

5.2.2 General:

- A proper implementation of the physics based approach would need adequate parameterisation of the inversion models. This requires fieldwork and sampling and laboratory analysis of the optical characteristics of the water column and *in situ* collection of a spectral library of the substratum. There is evidence that the spectral library collected on seagrass and macro-algae washed ashore tends to overestimate the actual reflectance of a canopy *in situ* as the spectral measurement on the beach is of a stack of macro-algae or seagrass leaves measured with the leaves lying flat, whereas the leaves actually float or sway in water thereby creating self shading. More research needs to be done on understanding the influence on the absolute reflectance of leaf orientation in underwater canopies.

- As fisherman do operate in some of these waters it may be useful to inventory the benthic material that is trawled to the surface, together with the most likely GPS position as that will provide ancillary information. Abalone or recreational divers could also be queried and asked to provide under water photographs. Another *in situ* sampling method that avoids having to get boats in to the water is to launch a lightweight unmanned underwater autonomous vehicle equipped with cameras or other optical equipment from the beach to provide *in situ* assessment in difficult to access waters.

- More knowledge is required on the substratum reflectance under sparse seagrass or macro-algae canopies. It would, for example, be useful to know how much detritus is present as that may colour the bottom reflectance a darker shade.

- A different approach to the model inversion, taking into account only spectral matching (α) instead of a magnitude match (αf) should be investigated to partially reduce the effect of the difference in albedo between spectral libraries and image spectra.

- By making use of the 25 years of Landsat data archives (now freely available from the United States Geological Service) it is feasible to perform a coarse level of change detection for these coasts. Detecting change in the size of sandy patches is feasible and maybe bathymetry and the ratio of seagrass to macro-algae, however less noisy data must be sourced for advancement of this methdology.

- It is advised to contact the Australian Hydrographic Service to ascertain whether the laser Airborne Depth Sounding System (LADS) has ever collected bathymetry data within these waters and if this data is available from the AHS.

REFERENCES

Adler-Golden, S.M., Bernstein, L.S., & Richtsmeier, S.C. (1998). Flaash, A Modtran4 Atmospheric Correction Package for Hyperspectral Data Retrievals and Simulations. In, AVIRIS Airborne Geoscience Workshop 1998 Pasadena, CA

Brando, V.E., Anstee, J.M., Wettle, M., Dekker, A.G., Phinn, S.R., & Roelfsema, C. (2009). A physics based retrieval and quality assessment of bathymetry from suboptimal hyperspectral data. Remote Sensing of Environment, 113, 755-770

Brando, V.E., & Dekker, A.G. (2003). Satellite hyperspectral remote sensing for estimating estuarine and coastal water quality. IEEE Trans.Geosci.Remote Sens., 41, 1378-1387

De Haan, J.F., & Kokke, J.M.M. (1996). Remote sensing algorithm development Toolkit I: Operationalization of atmospheric correction methods for tidal and inland waters. Report no. BCRS 96-16. Netherlands Remote Sensing Board, Delft.

De Haan, J.F., Kokke, J.M.M., Hoogenboom, H.J., & Dekker, A.G. (1997). An integrated toolbox for processing and analysis of remote sensing data of inland and coastal waters-atmopsheric correction. In, Fourth International Conference: Remote Sensing for Marine and Coastal Environments (pp. 1-215-211-222): ERIM

Hedley, J.D., Harborne, A.R., & Mumby, P.J. (2005). Technical note: Simple and robust removal of sun glint for mapping shallow water benthos. Int.J.Remote Sensing, 26, 6

Hochberg, E.J., Andréfouët, S., & Tyler, M.R. (2003). Sea surface correction of high spatial resolution Ikonos images to iprove bottom mapping in near-shore environments. IEEE Trans.Geosci.Remote Sens., 41, 1724-1729

Krause, K.S. (2004). Relative radiometric characterization and performance of the QuickBird high-resolution commercial imaing satellite. In W.L. Barnes & J.J. Butler (Eds.), Earth Observing Systems IX, (pp. 35-44),SPIE. Bellingham, WA

Krause, K.S. (2006). QuickBird relative radiometric performance and on-orbit long term trending. In J.J. Butler & J. Xiong (Eds.) Earth Observing Systems XI, SPIE. San Diego, CA.

Lee, Z., Carder, K.L., Mobley, C.D., Steward, R.G., & Patch, J.F. (1999). Hyperspectral remote sensing for shallow waters: 2. deriving bottom depths and water properties by optimization. Applied Optics, 38, 3831-3843

Lee, Z., Ivey, J.E., Carder, K.L., & Steward, R.G. (2000). Pure water absorption coefficient around 400nm: lab measured versus field observed. In proceedings of Ocean Optics XV, Monaco.

Lee, Z., Kendall, L.C., Chen, R.F., & Peacock, T.G. (2001). Properties of the water column and bottom derived from Airborne Visible Imaging Spectrometer (AVIRIS) data. Journal of Geophysical Research: Oceans, 106: 11639-11651

Lee, Z.P., Carder, K.L., Mobley, C.D., Steward, R.G., & Patch, J.S. (1998). Hyperspectral remote sensing for shallow waters. I. A semianalytical model. Applied Optics, 37, 6329-6338

Maritorena, S., Morel, A., & Gentili, B. (1994). Diffuse reflectance of oceanic shallow waters: influence of water depth and bottom albedo. Limnol.Oceanogr., 39, 1689-1703

Mobley, C.D., Sundman, L., Davis, C.O., Bowles, J.H., Downes, T.V., Leathers, R.A., Montes, M.J., Bisset, W.P., Kohler, D.D.R., Reid, R.P., Louchard, E.M., & Gleason, A. (2005). Interpretation of hyperspectral remote-sensing imagery by spectrum matching and look-up tables. Applied Optics, 44, 3576-3592

Moran, M.S., Bryant, R., Thome, K., Ni, W., Nouvellon, Y., Gonzalez-Dugo, M.P., & Qi, J. (2001). A refined empirical line approach for reflectance factor retrieval from Landsat-5 TM and Landsat-7 ETM+. Remote Sensing of Environment, 78, 71-82

Morel, A. (1974). Optical properties of pure water and pure sea water. In N.G. Jerlov & E.S. Nielsen (Eds.), Optical Aspects of Oceanography (pp. 1-24). London: Academic Press

Phinn, S., Roelfsema, C., Scarth, P., Dekker, A.G., Brando, V.E., Anstee, J.M., & Marks, A. (2005). An integrated remote sensing approach for adaptive management of complex coastal waters. Final Report - Moreton Bay Remote Sensing Tasks (MR2)

CRC for Coastal Zone, Estuary & Waterway Management. Technical Report No. 23. In (p. 132 p). Indooroopilly: CRC for Coastal Zone, Estuary & Waterway Management

Pope, R.M., & Fry, E.S. (1997). Absorption spectrum (380-700 nm) of pure water. II. Integrating cavity measurements. Appl.Opt., 36, 8710-8723

Vahtmae, E., & Kutser, T. (2008). Sun glint correction of airborne AISA images for mapping shallow-water benthos. In, IEEE/OES Us/EU-Baltic International Symposium (pp. 239-246). Tallinn, ESTONIA: IEEE

Wettle, M., & Brando, V.E. (2006). SAMBUCA - Semi-analytical model for Bathymetry, un-mixing and concentration assessment. . In, CSIRO Land and Water Science Report Canberra: CSIRO Land and Water

Wettle, M., Brando, V.E., & Dekker, A.G. (2004). A methodology for retrieval of environmental noise equivalent spectra applied to four Hyperion scenes of the same tropical coral reef. Remote Sensing of Environment, 93, 188-197

Wettle, M., Dekker, A., & Brando, V.E. (2005). Monitoring bleaching of tropical coral reefs from space. A feasibility study using a physics-based remote sensing approach. In: CSIRO Wealth from Oceans Flagship Program.

Contact Us
Phone: 1300 363 400
+61 3 9545 2176
Email: enquiries@csiro.au
Web: www.csiro.au

Your CSIRO

Australia is founding its future on science and innovation. Its national science agency, CSIRO, is a powerhouse of ideas, technologies and skills for building prosperity, growth, health and sustainability. It serves governments, industries, business and communities across the nation.